ERJ open research
THE BEST IN OPEN ACCESS BASIC, TRANSLATIONAL & CLINICAL RESPIRATORY RESEARCH

Early View

Original research article

Azithromycin alters spatial and temporal dynamics of airway microbiota in idiopathic pulmonary fibrosis

Pieter-Jan Gijs, Cécile Daccord, Eric Bernasconi, Martin Brutsche, Christian Clarenbach, Katrin Hostettler, Sabina A. Guler, Louis Mercier, Niki Ubags, Manuela Funke-Chambour, Christophe von Garnier

Please cite this article as: Gijs P-J, Daccord C, Bernasconi E, *et al*. Azithromycin alters spatial and temporal dynamics of airway microbiota in idiopathic pulmonary fibrosis. *ERJ Open Res* 2023; in press (https://doi.org/10.1183/23120541.00720-2022).

Azithromycin alters spatial and temporal dynamics of airway microbiota in idiopathic pulmonary fibrosis

*Pieter-Jan Gijs[a], *Cécile Daccord[a], Eric Bernasconi[a], Martin Brutsche[b], Christian Clarenbach[c], Katrin Hostettler[d], Sabina A. Guler[e], Louis Mercier[a], Niki Ubags[a], +Manuela Funke-Chambour[e] and +Christophe von Garnier[a]

Affiliations

[a] Division of Pulmonology, Department of Medicine, CHUV, Lausanne University Hospital, Lausanne, University of Lausanne, Switzerland
[b] Lung center, Kantonsspital St. Gallen, St. Gallen, Switzerland
[c] Division of Pulmonary Medicine, University Hospital of Zurich, Zurich, Switzerland
[d] Clinics of Respiratory Medicine, University Hospital Basel, Basel, Switzerland
[e] Department of Pulmonary Medicine, Inselspital, Bern University Hospital, Bern, Switzerland

* Shared first authorship
+ Shared last authorship

Corresponding Authors:

Niki Ubags, PhD
Division of Pulmonology, Department of Medicine, CHUV, Lausanne University Hospital, Lausanne, University of Lausanne, Switzerland
Email : Niki.Ubags@chuv.ch

Authors' contributions:

Conception and design: SG and MFC Funding acquisition: CD and MFC. Acquisition of data: PJG, EB, LM, CC, MB, KH, SG and MFC. Analysis and interpretation of data: PJG, EB, CD, NU, MFC and CVG. Drafting or revising of manuscript: PJG, EB, CD, NU, MFC and CVG. All authors critically revised and finally approved the manuscript.

Word count:

3958

Take home message:

In IPF, azithromycin alters the dynamics of the microbiota between the upper and lower airways and community turnover over time, with a decrease in richness without impacting the bacterial density.

Abstract

Background: High bacterial burden in lung microbiota predicts progression of idiopathic pulmonary fibrosis (IPF). Azithromycin (AZT) is a macrolide antibiotic known to alter the lung microbiota in several chronic pulmonary diseases and observational studies have shown a positive effect of azithromycin on mortality and hospitalization rate in IPF. However, the effect of AZT on lung microbiota in IPF remains unknown.

Methods: We sought to determine the impact of a three-month course of AZT on lung microbiota in IPF. We assessed sputum and oropharyngeal swab specimens from 24 adults with IPF included in a randomized controlled cross-over trial of a thrice-weekly 500 mg oral AZT. 16S rRNA gene amplicon sequencing and quantitative polymerase chain reaction (qPCR) were performed to assess bacterial communities. Antibiotic resistance genes (ARG) were assessed using real-time qPCR.

Results: AZT significantly decreased community diversity with a stronger and more persistent effect in lower airways (sputum). AZT treatment altered the temporal kinetics of the upper (oropharyngeal swab) and lower airway microbiota, increasing community similarity between the two sites for one month after macrolide cessation.
Patients with an increase in ARG carriage had lower bacterial density and enrichment of the genus *Streptococcus*. In contrast, patients with more stable ARG carriage had higher bacterial density and enrichment in *Prevotella*.

Conclusions: AZT caused sustained changes in the diversity and composition of the upper and lower airway microbiota in IPF, with effects on the temporal and spatial dynamics between the two sites.

Keywords: Microbiota; idiopathic pulmonary fibrosis; azithromycin; antibiotic resistance gene.

Introduction

Idiopathic pulmonary fibrosis (IPF) is a progressive and fatal interstitial lung disease of unknown origin and the most common and severe form of the idiopathic interstitial pneumonias(1,2).
In healthy subjects, the composition of the microbiota in the upper respiratory tract (URT) and lower respiratory tract (LRT) has considerable similarities(3). In the LRT, the influx of bacteria by microaspiration is counterbalanced by mucociliary clearance, resulting in a physiological turnover. Respiratory health is therefore associated with a dynamic turnover of the microbiota between the URT and the LRT.
Although alterations in the microbiota have not been found in lung tissue in end-stage IPF(4), converging evidence suggests that the spatial and temporal dynamics of the airway microbiota are disturbed during the disease course. In IPF, LRT microbiota is more abundant(5,6) and less diverse(7), suggesting either greater local growth, accumulation due to impaired clearance, or both. One consequence is greater dissimilarity between URT and LRT microbiota, with LRT microbiota carrying a majority of genes absent in the URT(8). This, alongside evidence from longitudinal studies on persistence of LRT microbiota disturbances(9), provides additional evidence for a lower microbiota turnover in IPF.
Preclinical data suggest that disruption of LRT microbiota precedes chronic lung epithelial injury and repair(7,10), potentially perpetuating inflammation(9). Bacterial load is currently the LRT microbiota feature most consistently associated with disease, in terms of progression, exacerbations and mortality. Bacterial load is higher in IPF patients than in healthy subjects, making it a potential therapeutic target(11). Although, antimicrobial treatment with doxycycline or co-trimoxazole in addition to standard care did not improve time to death or non-elective hospitalisation(12), the effects of microbiome alterations by disease or drug treatment are poorly understood.
A single-centre retrospective study showed good tolerance to prophylactic AZT in IPF patients, with fewer non-elective hospitalisations(13). Also, treatment with AZT during acute IPF exacerbations improved survival rates compared to fluoroquinolones in a retrospective single-centre study(14).
The impact of AZT on the respiratory microbiota in IPF is unknown. In patients with severe asthma and emphysema, multiple effects on the composition and structure of the LRT microbiota, as well as increased anti-inflammatory bacterial metabolites have been reported(15,16). This effect of AZT on LRT microbiota was independent of a decrease in bacterial load.
Acquired macrolide resistance is a global health concern and macrolide administration increases the carriage of macrolide-resistant bacteria in URT(17,18) and LRT(19). Higher carriage was observed after AZT for seven genes involved in antibiotic resistance, five of which associated with macrolide resistance, and two with tetracycline resistance(15). Additionally, the airway resistome positively correlates with bacterial load in chronic obstructive pulmonary disease (COPD)(20).

The aim of this study is to explore the impact of a three-month treatment of AZT on the airway microbiota of IPF patients.

Materials and Methods

Study population and sample collection

This study is a post hoc analysis of samples collected during the study conducted by Guler *et al*. (Clinical trial identifier: NCT02173145)(21). This previous study was a multi-centre, double-blind, randomised, placebo-controlled cross-over trial to determine the effect of AZT on chronic cough in IPF patients (see Supplementary materials for details).

Patients underwent a 12-week treatment period with oral AZT 500 mg 3 times per week, and a 12-week treatment period with placebo 3 times per week in randomised order. The two periods were separated by a 4-week washout period.

Sputum samples, either expectorated or induced by inhalation of a 3% sodium chloride solution, and oropharyngeal swab (OPS) samples were collected both before and after AZT and placebo periods, and an additional specimen was collected after the 4-week washout period following the second treatment period. Samples were stored at -80°C until analysis. The study design and detailed sample collection are presented in **Figure E1** in the Supplementary materials (see Supplementary materials for details of study population and sample collection).

DNA extraction and 16S rRNA gene amplicon quantification

Sputum and OPS samples were treated with dithiothreitol to homogenise the mucosal phase and DNA was extracted using the DNeasy UltraClean microbial kit (Qiagen, Hilden, Germany), with inclusion of a lysozyme digestion step (see details in Supplementary materials).

Negative controls (N = 11) underwent the same procedure and included blank swabs, blank sputum collection tubes, as well as blank DNA extractions (reagent control).

To obtain a proxy of bacterial density, we determined the copy numbers of the 16S rRNA gene by qPCR using previously reported primers specific to panbacteria(22) (see **Supplementary Table E1** for full sequences). Standard curves were obtained using purified amplicon products.

Bacterial 16S rRNA gene amplicon sequencing

Amplicon sequencing targeted the V1-V2 region of the 16S rRNA gene with primers F-27 and R-338 (see **Supplementary Table E1** for full sequences and Supplementary materials for details). Amplification was performed using the Accuprime Taq DNA Polymerase High Fidelity kit (Invitrogen, Waltham, MA). No-template PCR reaction controls (N = 2) were included. Libraries were loaded onto an Illumina MiSeq using pairwise chemistry, generating 250 × 2 read lengths (Lausanne Genomic technologies facility, University of Lausanne, Switzerland).

Analysis of antibiotic resistance gene carriage

Quantification of antibiotic resistance genes (ARG) carriage targeting 23S ribosomal RNA methyltransferases (*erm*(B) and *erm*(F)), ATP-binding cassette ribosomal protection protein (*mel* and *msr*[E]), major facilitator superfamily antibiotic efflux pump (*mef*), and tetracycline-resistant ribosomal protection proteins (*tet*[M] and *tet*[W]) was performed on sputum specimens using dye-based (SsoAdvanced Universal SYBR Green, Bio-Rad) or probe-based real-time PCR assays, using primer pairs, probes and conditions previously described(15). The copy numbers of resistance genes per sample were normalised relative to the copy numbers of the 16S rRNA gene. To obtain a synthetic picture of ARG carriage per sample, the counts obtained for each individual gene were scaled from 0 to 1 to provide equal importance to each gene, and the cumulative counts were reported.

Bioinformatics and statistical analysis

All analyses were performed in R version 4.1.0(23). Demultiplexing, removal of chimeric and short reads, single-base resolution of reads into amplicon sequence variants (ASVs) using the Divisive Amplicon Denoising Algorithm 2 (DADA2) algorithm(24), and taxonomic annotation using the SILVA database(25) were performed using a dedicated pipeline available at https://github.com/chuvpne/dada2-pipeline. Contaminant screening was performed using decontam package (**Figure E2**). Subsequent analyses were performed on a rarefied dataset at a sequencing depth of 10,055 (**Figures E3, E4 and E5;** see Supplementary materials for details on processing and quality control).

Multiple group comparisons were made using Kruskal-Wallis test with Dunn's post hoc test and Holm's adjustment. The Wilcoxon signed-rank test was used to compare paired data. In all tests, we considered an alpha significance level of 0.05[26].
Comparisons of proportions of ASVs represented only in one condition or shared between two conditions were assessed using the chi-square goodness-of-fit test.
To test for differences in microbiota composition between the different phases of AZT treatment, we used a matrix built on either unweighted or weighted UniFrac distance and conducted a Permutational Multivariate Analysis of Variance (PERMANOVA) with 999 permutations.
R scripts are available at https://github.com/CHUVpulmonology/Airway_microbiota-Lung_fibrosis-Azithromycin. The original sequencing data and the starting data for the analyses in R are available at 10.5281/zenodo.7065053.

Results

Study cohort

Of the 25 patients who completed randomization, 12 were initially randomized to intervention and 13 to placebo. 20 patients completed the study. The Consolidated Standards of Reporting Trials (CONSORT) diagram is shown in **Figure E6** in Supplementary materials**.**
24 patients had at least one specimen, with a total of 67 sputum and 90 OPS specimens. **Table 1** shows patient demographics and clinical characteristics.
Bacterial quantification, 16S rRNA gene amplicon sequencing and ARG analysis were performed on all specimens, except on 1 OPS specimen with insufficient DNA. 10 OPS specimens not meeting the 10,055 read threshold were excluded from further sequencing analysis (**Figure E3** see Supplementary materials). Finally, 67 sputum and 79 OPS specimens were analyzed.
To investigate temporal changes in respiratory microbiota linked to AZT, we distinguished five treatment phases: *PreAZT* for specimens collected before the start of AZT treatment, available only in patients who started with placebo (N=35; sputum=14; OPS=21), *StartAZT* for specimens collected at the beginning of AZT (N=31; sputum=15; OPS=16), *EndAZT* for specimens collected at the end of AZT (N=23; sputum=12; OPS=11), *PostAZT_1 month* for specimens collected 1 month after the end of treatment (N=32; sputum=14; OPS=18) and *PostAZT>=3 months* for specimens collected 3 months or more after the end of AZT (N=25; sputum=12; OPS=13).

The respiratory microbiota of IPF patients is distinct from environmental noise

As our study used low volume specimens from body sites with low microbial biomass, it was vulnerable to environmental noise(26). However, we detected a significantly higher bacterial density (median, interquartile range [IQR]) in both LRT ($2x10^5$, $5.4x10^4$ - $4.5x10^5$) ($p < 0.001$; **Figure E7a**) and URT ($1.7x10^5$, $6.5x10^4$ - $7.8x10^5$) ($p < 0.001$; **Figure E7b**) specimens compared to procedural controls ($4x10^4$, $1.4x10^4$ – $5.6x10^4$).
Rank abundance analysis further showed that the dominant bacteria were mostly different in patient samples versus controls (**Figure E7c**).

The upper and lower airway microbiota of IPF patients is altered after AZT treatment

We found no difference in bacterial density between the different treatment phases in either LRT ($p = 0.95$) or URT ($p = 0.19$; **Figure 1**), but we observed a decrease in community richness after AZT, with a stronger and more persistent effect in the LRT ($p = <0.001$) compared to the URT ($p = 0.029$; **Figure 2a**). A decrease in bacterial phylogenetic diversity was also observed in LRT ($p = <0.001$) and at the limit of significance in URT ($p = 0.053$), without reverting to the pre-treatment level until the end of the observation period for LRT and more transiently for URT (**Figure 2b**). This decrease in alpha diversity between the start and end of AZT treatment, and the overall kinetics throughout the study, were confirmed by intra-individual (**Figure E8**) and genus-level (**Figure E9**) analyses.
In contrast, evenness increased transiently after treatment in URT only ($p <0.001$; **Figure 2c**), while Shannon diversity index reflected the effects of AZT on richness (**Figure 2d**).
We observed no overall variation in the dominance of core community ASVs (i.e. abundance greater than 0.1% in 50% of samples) in both LRT ($p = 0.29$) and URT ($p = 0.99$; **Figure E10**), suggesting that the impact of AZT treatment did not primarily target the most abundant and prevalent bacteria.
Principal coordinate analysis (PCoA) based on unweighted UniFrac distance, which accounts for phylogeny, further supported variations in the microbiota present before and at the start of treatment compared to that

found at the end and after treatment, with marked changes in LRT (p = 0.006; **Figure E11a**), but at the limit of significance in URT (p = 0.053; **Figure E11b**).

Together, these results show a broad impact of AZT on the respiratory microbiota of IPF patients.

AZT treatment reduces spatial dissimilarity between URT and LRT microbiota and affects their temporal dynamics

Based on unweighted UniFrac distance, bacterial communities in URT and LRT were distinct (**Figure 3a**). Per-patient comparisons showed greater similarity between URT and LRT samples at the end of AZT treatment, with the effect persisting one month after treatment and attenuating thereafter (**Figure 3b**). The impact of treatment was confirmed to be mainly on taxa of relatively low abundance, as indicated by a smaller effect based on weighted Unifrac distance compared to unweighted Unifrac distance (**Figure E12, compare with Figure 4b**). This treatment-related decrease in dissimilarity between the two sites was also observed at genus level (**Figure E13a**). Divergence of the microbiota between the two sites was driven by ASVs present only in LRT, more numerous than those present only in URT or shared between the two sites, in each treatment phase ($p < 0.05$ except at 4 months or more after treatment). The transient decrease in the divergence between URT and LRT microbiota after AZT was associated with a non-significant decrease in the proportion of ASVs represented in LRT only, and a marginal increase in the number of ASVs shared by both sites **(Figure 3c).**

Analysis of samples from IPF patients first receiving placebo allowed quantification of bacterial turnover over a three-month period in the absence of AZT. We found a total of 40% ASVs retained in URT, and 45% in LRT (**Figure 3d, left diagrams**).

AZT treatment altered the temporal dynamics of the airway microbiota, with fewer ASVs present at the end compared to the start of AZT treatment in LRT ($p < 0.001$) and URT ($p = 0.02$). In LRT, the number of newly acquired ASVs was also lower than the number of retained ASVs ($p = 0.005$), in contrast to the observations in patients receiving placebo first (**Figure 3d, middle diagrams**).

However, the bacterial turnover after treatment was increased compared to the placebo first group, with numbers of newly acquired ASVs exceeding those of cleared ASVs in the LRT ($p = 0.045$) but not reaching significance in the URT ($p = 0.059$; **Figure 3d, right diagrams**). The observations were confirmed at genus level (**Figure E13b**).

We observed that bacteria cleared from LRT during treatment, which accounted for 20.7% (median, IQR 13.6-27.6) of the local community at the start of treatment, were already present in this site at 16.5% (median, IQR 11.2-28.6) relative abundance at least four months before treatment started. The effect of treatment on these bacteria was long-lasting, with only partial resilience five months after the end of treatment. These same bacteria followed similar kinetics in URT, with a relative abundance of 12.7% (median, IQR 11.2-28.6) in the 4 months prior to the start of treatment and then decreasing to 0.08% (median, IQR 0.01-0.1) at the end of treatment (**Figure 4a**).

Bacteria acquired in LRT during treatment were represented in some cases at low levels during the four months prior to treatment. Their local relative abundance was highest at the end of treatment, without reaching the levels of bacteria cleared by the treatment, before decreasing during the 5 months following the end of treatment. These same bacteria were also poorly represented in URT prior to treatment (median 0%; IQR 0-0.09%). At the end of treatment, their local relative abundance had also increased (median 2.9%; IQR 0.8-3.4%), and, for some patients, these bacteria remained detectable in URT for up to 5 months after the end of treatment (**Figure 4b**).

Taken together, these observations indicate marked changes in the spatial distribution and temporal dynamics of the airway microbiota of IPF patients secondary to AZT treatment.

Changes in the composition of LRT microbiota correlate with antibiotic resistance gene carriage

We next investigated whether alterations in respiratory microbiota during AZT treatment were related to ARG acquisition, focusing on LRT and previously described target genes(15). We observed that ARG carriage was limited to a minority of LRT samples and ASVs (**Figure 5a**) and that almost all samples with ARG were collected at the end of AZT treatment or later (**Figure 5b**). This was confirmed by longitudinal within-patient analysis, which showed a peak in total ARG carriage at the end of AZT treatment, with substantial inter-individual differences in post-treatment kinetics (**Figure 5c**).

To investigate the implications for LRT microbiota of an increase in ARG carriage, we separated patients with LRT samples available at the start and end of AZT treatment (N = 10) into two groups of five patients according to the median change in the cumulative sum of seven pooled ARG (median fold-change = 3.8; **Figure E14**).
This revealed an association between ARG carriage and bacterial density, with a higher density in patients with stable resistance compared with those with increased resistance during AZT treatment ($p < 0.001$) (**Figure 6a)**. However, there was no change in bacterial density between the different treatment phases, whether ARG carriage status was stable or increased (**Figure E15**).
We observed changes in the composition of LRT microbiota between the start and end of treatment, depending on resistance status. Specifically, double PCoA focused on the 15 most abundant genera showed that AZT treatment was associated with a shift in composition influenced by *Prevotella_7* abundance, in all patients with stable resistance and only in one patient with increased resistance. In contrast, the other four patients with increased ARG carriage showed compositional changes mainly driven by *Streptococcus* (**Figure 6b and c**).
Genus abundance analysis during treatment confirmed an increase in *Prevotella_7* and a decrease in *Streptococcus* in patients with stable resistance, and an increase in *Streptococcus* in 4 out of the 5 patients with increased resistance (**Figure E16a and b).** Finally, enrichment of *Prevotella_7* in patients with stable resistance during treatment ($p = 0.0064$; **Figure E16c**), and of *Streptococcus* in those with increased resistance ($p = 0.002$; **Figure E16d**), was also observed when all samples of these patients were considered, including those taken before the start or after the end of treatment.
Finally, of the 25 genera with the highest number of ASVs lost during treatment, *Treponema_2* and *Fretibacterium* were represented in both patients with stable and increasing resistance status but were absent in a similar ranking of ASVs acquired during treatment (**Figure E17a** and **b**).
As a result, these genera were significantly less prevalent and less abundant at the end of treatment and in the following months, with no or moderate signs of resilience (for *Fretibacterium* and *Treponema_2*, respectively). On the contrary, *Pseudopropionibacterium* was represented among the ASVs acquired during treatment, with a prevalence still preserved one month later (**Figure 7**)

Together, these observations link the resistome to the composition of LRT microbiota, with a direct correlation with local bacterial density, but without change in lung function during the study period (**Figure E18**)[28].

Discussion

This study provides valuable insight on the spatial and temporal distribution of the respiratory microbiota in IPF by comparing URT and LRT, microbial turnover, and the impact of AZT on these dynamics.
Our findings suggest an attenuating effect of AZT on airway ecological disruption but also disturbance in LRT through a decrease in community diversity and an increase of potential pathogenic community members.
These effects persisted up to five months after the end of treatment, possibly due to AZT retention in lung macrophages(27). No changes in clinical status were observed during the study period(21).

URT and LRT communities in our cohort of IPF patients differed significantly, as in other chronic respiratory diseases(28,29), with microbial richness in LRT exceeding that in URT, which contrasts with the situation in healthy subjects.
Greater decrease in microbial richness in LRT versus URT during AZT treatment, paralleled by a diminishing phylogenetic dissimilarity between microbiota of the two sites, suggests that treatment decreases airway ecological disturbance. Our observation of no concomitant decrease in bacterial density could imply that the numerous taxa cleared were replaced by a smaller number of taxa already present and becoming more dominant. As increased dominance may alter the bacterial impact on host, it is often interpreted as being harmful, but little is known about the threshold for detrimental dominance, which depends on bacteria and the clinical context.

Further evidence of AZT treatment effects was investigated by assessing bacterial temporal dynamics. In the absence of AZT, bacterial turnover was lower in the LRT compared to the URT. Combined with excessive microbial richness in LRT, this suggests a local persistence of bacteria potentially harmful to the host. AZT treatment had two effects on this microbiota dynamic, namely by eliminating taxa (decrease in richness) and by preventing the acquisition of new taxa. However, these effects vanished progressively during the months following treatment.

The treatment-induced decrease in richness and phylogenetic diversity of the LRT microbiota was linked to a compositional change[15,16] mainly driven by a mutually exclusive increase in relative abundance of the two predominant genera in IPF lung, *Streptococcus* (Gram-positive *Firmicutes*) and *Prevotella* (Gram-negative *Bacteroidetes*). Enrichment of these genera was consistent with the development of macrolide resistance previously described in cystic fibrosis(30,31). The difference we observed with the increase in ARG carriage during AZT treatment when either of these genera predominated suggests that different mechanisms may be present[15]. While *Streptococcus* enrichment was associated with a marked increase in ARG carriage (in 4 out of 4 patients), *Prevotella* enrichment was linked to more stable ARG carriage (in 5 out of 6 patients). *Prevotella* acquisition of AZT resistance could be due to carriage of genes not listed in our targets, although we included the most likely candidates based on a previous metagenomic study of AZT treatment in severe asthma(15).
A larger sample size will be necessary to strengthen conclusions and to perform in-depth analysis to determine whether carriage of genes involved in tetracycline versus macrolide resistance is associated with different bacteria.

Although patients remained clinically stable during the study period, it is difficult to predict the impact of even a relatively transient predominance of *Streptococcus* or *Prevotella* on lung health. Both genera include commensal species that can act as opportunistic pathogens under permissive conditions. Some members of *Streptococcus* have been associated with IPF progression(6). *Prevotella* are maintained at low levels in the healthy lung, where they establish a subclinical level of inflammation favoring immune surveillance(3). However, their abundance is increased in IPF where they can become predominant(32). Furthermore, *Prevotella* are involved in several inflammatory diseases(33), including periodontitis, with a possible impact on the frequency of exacerbations in COPD(34). Accordingly, preclinical evidence suggests that *Prevotella* predominance in the airways promotes pulmonary fibrosis through a mechanism involving IL-17B(35). Decreased microbial diversity in IPF, such as observed with the predominance of *Streptococcus* or *Prevotella*, has previously been associated with increased alveolar concentrations of pro-inflammatory cytokines and profibrotic growth factors(10).
Further studies are required to determine the relationship between alterations of microbiota and gene expression in the airways during AZT treatment.

Our study has several limitations. i) We report an association between AZT and ARG carriage, but separate analysis of microbiota by amplicon sequencing and ARG carriage by qPCR does not allow us to identify bacteria that acquire resistance during treatment. Genome-wide metagenomic analyses would answer this question. ii) The absence of a healthy control group prevented us from assessing whether disruption of the airway microbiota by AZT is specific for IPF. iii) The use of sputum to sample the proximal lower airways in non-suppurative airway disease such as IPF is associated with a risk of cases being contaminated by saliva. Although to limit this risk in patients unable to expectorate, we used induction by instillation of hypertonic saline, the latter sampling method was reported to return differences in the composition of the LRT microbiota compared to spontaneous sputum in one third of patients in the COPD setting(36). However, the same study found no difference in alpha diversity between spontaneous and induced sputum[37]. iv) We defined bacterial turnover in this cohort of IPF patients by investigating the acquisition or loss of AVSs during the pre-treatment period in patients receiving placebo first. However, some of this variation over time is bound to be related to an artificial inflation of alpha diversity when measured on the basis of ASVs(37) and randomness related to sequencing depth, rarefaction and sequencing of low-biomass samples(38). The consistent results of the genus-level analyses suggest that this limitation plays a reasonably restricted role. v) Finally, our observations are based on the available specimens of 24 well-characterized IPF patients, but the size of the cohort limits the generalizability of our findings which call for larger studies.

Notwithstanding, this study provides the best available evidence on the effect of AZT on IPF airway microbiota. We report that AZT alters the spatial and temporal dynamics of airway microbiota in IPF patients with a decline in richness and phylogenetic diversity in URT and LRT, without impact on bacterial density. The AZT impact is characterized by increased *Prevotella* or *Streptococcus* abundance and persists with partial resilience five months after treatment. Also, ARG carriage is increased in half of patients in the presence of *Streptococcus* predominance.
In conclusion, this study provides novel insights into airway ecology disturbances in IPF by longitudinal sampling of URT and LRT and expands on previous knowledge from studies in distal LRT. From a clinical care perspective this approach encourages non-invasive sampling of more than one respiratory tract site.

Acknowledgements

We thank the patients who participated in the study and the study nurses from Bern, Basel, St. Gallen and Zurich for their work and data acquisition. We also thank the Lung Association of the Canton of Vaud (Ligue Pulmonaire Vaudoise, LPV) and the Research Fund of the Swiss Lung Association, Bern for financial support.
16S rRNA sequencing was performed at the Lausanne Genomic Technologies Facility, University of Lausanne, Switzerland (https://www.unil.ch/gtf/en/home.html).

Characteristics	Study cohort (N=25)
Age, years	67 (8)
Sex, men	23 (92%)
Previous smokers	17 (68%)
Current smoker	1 (4%)
Diagnosis	
Definite UIP pattern on HRCT	18 (72%)
Surgical lung biopsy available	12 (48%)
Multidisciplinary team discussion performed	19 (76%)
Treatment	
Pirfenidone	9 (36%)
Nintedanib	11 (44%)
Proton pump inhibitor	13 (52%)
Oxygen therapy	9 (36%)
Pulmonary function tests	
TLC, % predicted	60 (12)
FVC, % predicted	65 (16)
FEV1/FVC, %	86 (7)
DL_{CO}, % predicted	43 (16)
Comorbidities	
Chronic rhinitis	8 (32%)
Sinusitis	2 (8%)
Gastroesophageal reflux disease	4 (16%)
Cardiac disease	11 (44%)
Pulmonary hypertension	3 (12%)
Diabetes	4 (16%)

Table 1. Demographics and clinical characteristics of study cohort(21)
Abbreviations: UIP = usual interstitial pneumonia; HRCT = high-resolution computed tomography; TLC = total lung capacity; FVC = forced vital capacity; FEV1 = forced vital capacity in 1 second; DL_{CO} = diffusing capacity of the lung for carbon monoxide.
Values are presented as frequency and percentage or mean and standard deviation (SD)

References

1. Maher TM, Wells AU, Laurent GJ. Idiopathic pulmonary fibrosis: multiple causes and multiple mechanisms? *Eur Respir J* **30**, 835–839 (2007).
2. Raghu, G, Remy-Jardin M, Myers JL *et al.* Diagnosis of Idiopathic Pulmonary Fibrosis An Official ATS/ERS/JRS/ALAT Clinical Practice Guideline. *Am J Respir Crit Care Med* **198**, 44–68 (2018).
3. Bassis CM, Erb-Downward JR, Dickson RP *et al.* Analysis of the upper respiratory tract microbiotas as the source of the lung and gastric microbiotas in healthy individuals. *mBio* **6**, (2015).
4. Kitsios GD, Rojas M, Kass DJ *et al.* Microbiome in lung explants of idiopathic pulmonary fibrosis: a case-control study in patients with end-stage fibrosis. *Thorax* **73**, 481–484 (2018).
5. Molyneaux PL, Cox MJ, Willis-Owen SA *et al.* The role of bacteria in the pathogenesis and progression of idiopathic pulmonary fibrosis. *Am J Respir Crit Care Med* **190**, 906–913 (2014).
6. Han MK, Zhou Y, Murray S *et al.* Lung microbiome and disease progression in idiopathic pulmonary fibrosis: An analysis of the COMET study. *Lancet Respir Med* **2**, 548–556 (2014).
7. Takahashi Y, Saito A, Chiba H *et al.* Impaired diversity of the lung microbiome predicts progression of idiopathic pulmonary fibrosis. *Respir Res* **19**, 1–10 (2018).
8. Tong X, Su F, Xu X *et al.* Alterations to the lung microbiome in idiopathic pulmonary fibrosis patients. *Front Cell Infect Microbiol* **9**, 149 (2019).
9. Molyneaux PL, Willis-Owen SAG, Cox MJ *et al.* Host-Microbial Interactions in Idiopathic Pulmonary Fibrosis. *Am J Respir Crit Care Med* **195**, 1640–1650 (2017).
10. O'Dwyer DN, Ashley SL, Gurczynski SJ *et al.* Lung Microbiota Contribute to Pulmonary Inflammation and Disease Progression in Pulmonary Fibrosis. *Am J Respir Crit Care Med* **199**, 1127–1138 (2019).
11. Invernizzi R, Barnett J, Rawal B *et al.* Bacterial burden in the lower airways predicts disease progression in idiopathic pulmonary fibrosis and is independent of radiological disease extent. *Eur Respir J* **55**, (2020).
12. Martinez FJ, Yow E, Flaherty KR *et al.* Effect of Antimicrobial Therapy on Respiratory Hospitalization or Death in Adults With Idiopathic Pulmonary Fibrosis: The CleanUP-IPF Randomized Clinical Trial. *JAMA* **325**, 1841–1851 (2021).
13. Macaluso C, Maritano Furcada J, Alzaher O *et al.* The potential impact of azithromycin in idiopathic pulmonary fibrosis. *Eur Respir J* **53**, (2019).
14. Kawamura K, Ichikado K, Yasuda Y *et al.* Azithromycin for idiopathic acute exacerbation of idiopathic pulmonary fibrosis: A retrospective single-center study. *BMC Pulm Med* **17**, (2017).
15. Taylor SL, Leong LEX, Mobegi FM *et al.* Long-Term Azithromycin Reduces Haemophilus influenzae and Increases Antibiotic Resistance in Severe Asthma. Am J Respir Crit Care Med. **200(**3):309-317 (2019).
16. Segal LN, Clemente JC, Wu BG *et al.* Randomised, double-blind, placebo-controlled trial with azithromycin selects for anti-inflammatory microbial metabolites in the emphysematous lung. *Thorax* **72**, 13–22 (2017).
17. Kastner U, Guggenbichler JP. Influence of macrolide antibiotics on promotion of resistance in the oral flora of children. *Infection* **29**, 251–256 (2001).
18. Choo JM, Abell GCJ, Thomson R *et al.* Impact of Long-Term Erythromycin Therapy on the Oropharyngeal Microbiome and Resistance Gene Reservoir in Non-Cystic Fibrosis Bronchiectasis. *mSphere* **3**, (2018).
19. Altenburg J, de Graaff CS, Stienstra Y *et al.* Effect of azithromycin maintenance treatment on infectious exacerbations among patients with non-cystic fibrosis bronchiectasis: the BAT randomized controlled trial. *JAMA* **309**, 1251–1259 (2013).
20. Ramsheh MY, Haldar K, Bafadhel M *et al.* Resistome analyses of sputum from COPD and healthy subjects reveals bacterial load-related prevalence of target genes. *Thorax* **75**, 8–16 (2020).
21. Guler SA, Clarenbach C, Brutsche M *et al.* Azithromycin for the Treatment of Chronic Cough in Idiopathic Pulmonary Fibrosis: A Randomized Controlled Crossover Trial. *Ann Am Thorac Soc* **18**, 2018–2026 (2021).
22. Bacchetti De Gregoris T, Aldred N, Clare AS *et al.* Improvement of phylum- and class-specific primers for real-time PCR quantification of bacterial taxa. *J Microbiol Methods* **86**, 351–356 (2011).
23. R Core Team (2021). R: A language and environment for statistical computing. R Foundation for Statistical Computing, Vienna, Austria.

24. Callahan BJ, McMurdie PJ, Rosen MJ *et al.* DADA2: High-resolution sample inference from Illumina amplicon data. *Nature Methods 2016 13:7* **13**, 581–583 (2016).
25. Quast C, Pruesse E, Yilmaz P *et al.* The SILVA ribosomal RNA gene database project: improved data processing and web-based tools. *Nucleic Acids Research* **41**, D590 (2013).
26. Salter SJ, Cox MJ, Turek EM *et al.* Reagent and laboratory contamination can critically impact sequence-based microbiome analyses. *BMC Biol* **12**, 1–12 (2014).
27. Aubert JD, Juillerat-Jeanneret L, Fioroni P *et al.* Function of human alveolar macrophages after a 3-day course of azithromycin in healthy volunteers. *Pulm Pharmacol Ther* **11**, 263–269 (1998).
28. Willner D, Haynes MR, Furlan M *et al.* Spatial distribution of microbial communities in the cystic fibrosis lung. *ISME J* **6**, 471–474 (2012).
29. Venkataraman A, Bassis CM, Beck JM *et al.* Application of a neutral community model to assess structuring of the human lung microbiome. *mBio* **6**, (2015).
30. Webb KA, Olagoke O, Baird T *et al.* Genomic diversity and antimicrobial resistance of Prevotella species isolated from chronic lung disease airways. *Microb Genom* **8**, 000754 (2022).
31. Tazumi A, Maeda Y, Goldsmith CE *et al.* Molecular characterization of macrolide resistance determinants [erm(B) and mef(A)] in Streptococcus pneumoniae and viridans group streptococci (VGS) isolated from adult patients with cystic fibrosis (CF). *J Antimicrob Chemother* **64**, 501–506 (2009).
32. Dickson RP, Huffnagle GB, Flaherty KR *et al.* Radiographic honeycombing and altered lung microbiota in patients with idiopathic pulmonary fibrosis. *Am J Respir Crit Care Med* **200**, 1544–1547 (2019).
33. Larsen JM. The immune response to Prevotella bacteria in chronic inflammatory disease. *Immunology* **151**, 363–374 (2017).
34. Kelly N, Winning L, Irwin C *et al.* Periodontal status and chronic obstructive pulmonary disease (COPD) exacerbations: a systematic review. *BMC Oral Health* **21**, 1–11 (2021).
35. Yang D, Chen X, Wang J *et al.* Dysregulated Lung Commensal Bacteria Drive Interleukin-17B Production to Promote Pulmonary Fibrosis through Their Outer Membrane Vesicles. *Immunity* **50**, 692-706.e7 (2019).
36. Tangedal S, Aanerud M, Grønseth R *et al.* Comparing microbiota profiles in induced and spontaneous sputum samples in COPD patients. *Respir Res* **18**, 1–9 (2017).
37. Schloss PD. Amplicon Sequence Variants Artificially Split Bacterial Genomes into Separate Clusters. *mSphere* **6**, (2021).
38. Erb-Downward JR, Falkowski NR, D'Souza JC *et al.* Critical Relevance of Stochastic Effects on Low-Bacterial-Biomass 16S rRNA Gene Analysis. *mBio* **11**, 1–12 (2020).

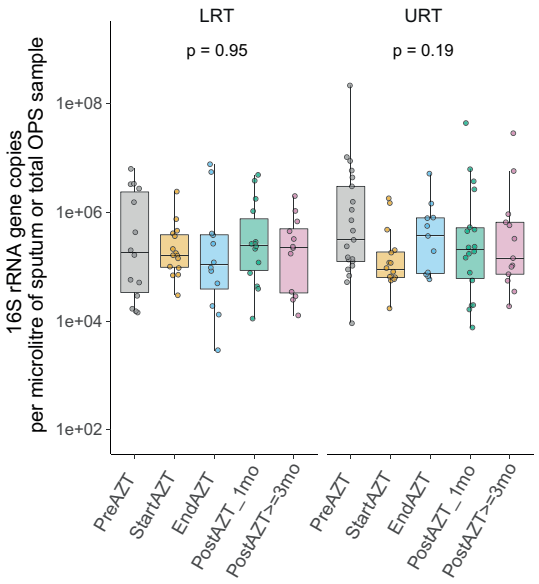

Figure 1. qPCR determination of 16S rRNA gene copy number per microlitre of sputum or total OPS showing no significant change in bacterial density during the different phases of the study. Middle lines, boxes and whiskers represent the median, interquartile range (IQR) and 1.5 times IQR respectively. Dots represent samples. Kruskal-Wallis with Dunn's post hoc test.
Abbreviations: qPCR = quantitative polymerase chain reaction; OPS = oropharyngeal swab; LRT = lower respiratory tract; URT = upper respiratory tract; AZT = azithromycin

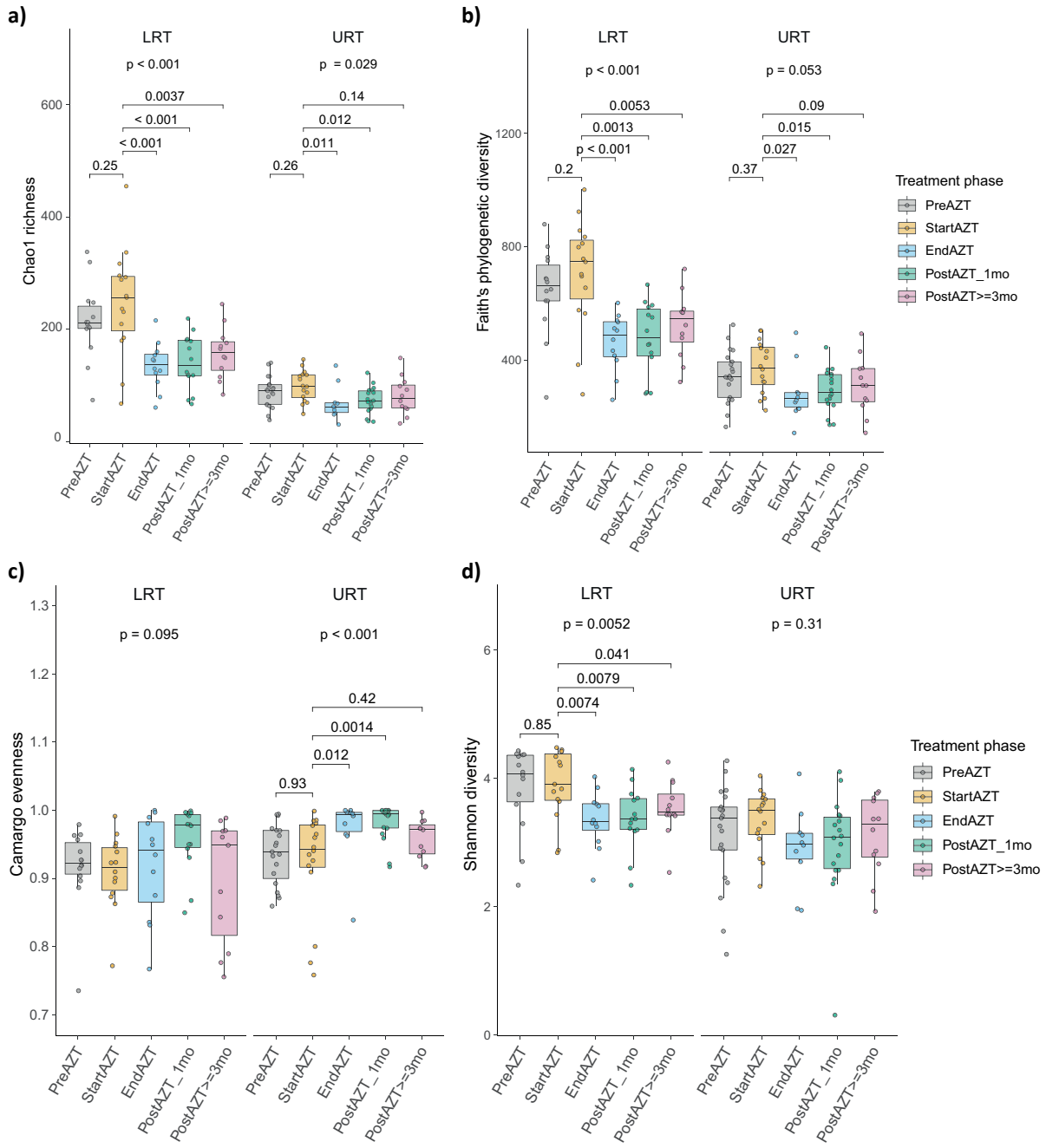

Figure 2. Decrease in community diversity after AZT treatment. (*a* to *d*) Alpha diversity metrics showing a decrease in Chao1 richness (*a*) and Faith's diversity (*b*) during AZT treatment in LRT and URT, an increase in Camargo evenness in URT (*c*), and a decrease in Shannon diversity in LRT (*d*). In all box plots, the middle line, box and whiskers represent the median, interquartile range (IQR) and 1.5 times the IQR, respectively. Dots represent samples. Kruskal-Wallis with Dunn's post hoc test.
Abbreviations: AZT = azithromycin; LRT = lower respiratory tract; URT = upper respiratory tract

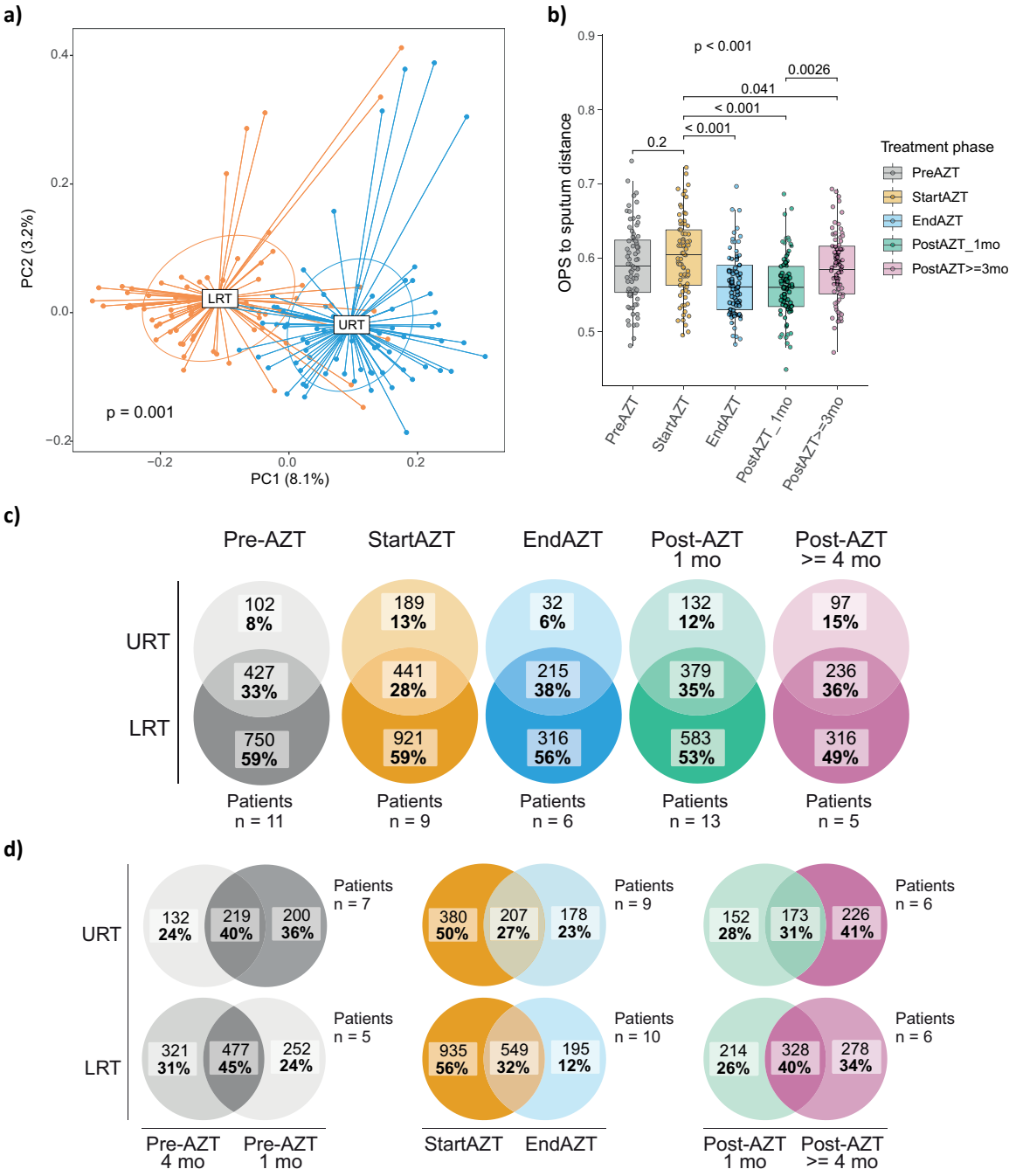

Figure 3. AZT treatment reduces dissimilarity between LRT and URT microbiota. (*a*) PCoA based on unweighted UniFrac distance showing an overall difference in bacterial community composition between URT and LRT. (*b*) Unweighted UniFrac distance calculated for each treatment phase between each OPS sample and the centroid obtained from the corresponding set of sputum samples. (*c*) Venn diagrams of the total numbers and proportion of ASVs represented in either the LRT or URT alone, or in both sites, showing that the decrease in dissimilarity between the LRT and URT microbiota during treatment was in part driven by a decrease in the proportion of ASVs present in the LRT alone.(*d*) Venn diagrams of the total numbers and proportion of ASVs represented either at the start, at the end or retained over a 3-month time window, showing treatment-induced alterations in the temporal dynamics of the LRT and URT microbiota. Significance tested using PERMANOVA (a) or Kruskal-Wallis with Dunn's post hoc test.

Abbreviations: AZT = azithromycin; LRT = lower respiratory tract; URT = upper respiratory tract; PCoA = principal coordinate analysis; OPS = oropharyngeal swab; ASVs = amplicon sequence variants

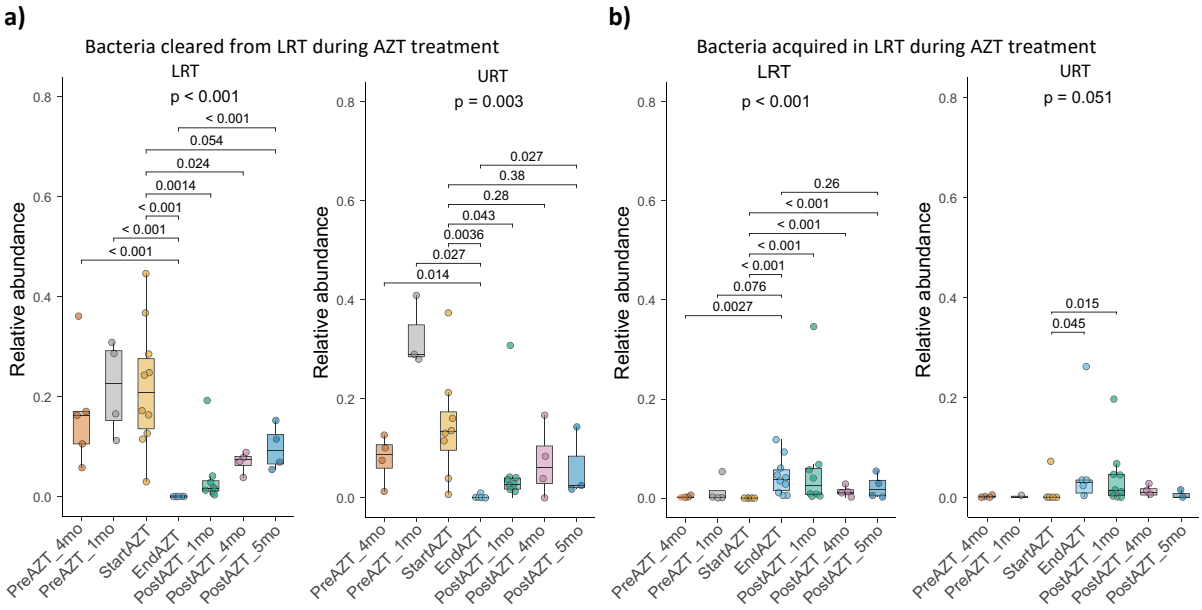

Figure 4. Longitudinal changes in the relative abundance of bacteria cleared (*a*) or acquired (*b*) in the LRT during AZT treatment, showing different magnitudes of change in relative abundance between cleared and acquired bacteria, and similar kinetics between LRT and URT. The relative abundance reported is the proportion of all ASVs lost (i.e. no reads at the end of treatment) or acquired (i.e. no reads at the start of treatment) during treatment, relative to the abundance of total ASVs per sample. Middle lines, boxes and whiskers represent the median, interquartile range (IQR) and 1.5 times IQR respectively. Dots represent samples. Kruskal-Wallis with Dunn's post hoc test.
Abbreviations: LRT = lower respiratory tract; AZT = azithromycin; URT = upper respiratory tract; ASVs = amplicon sequence variants

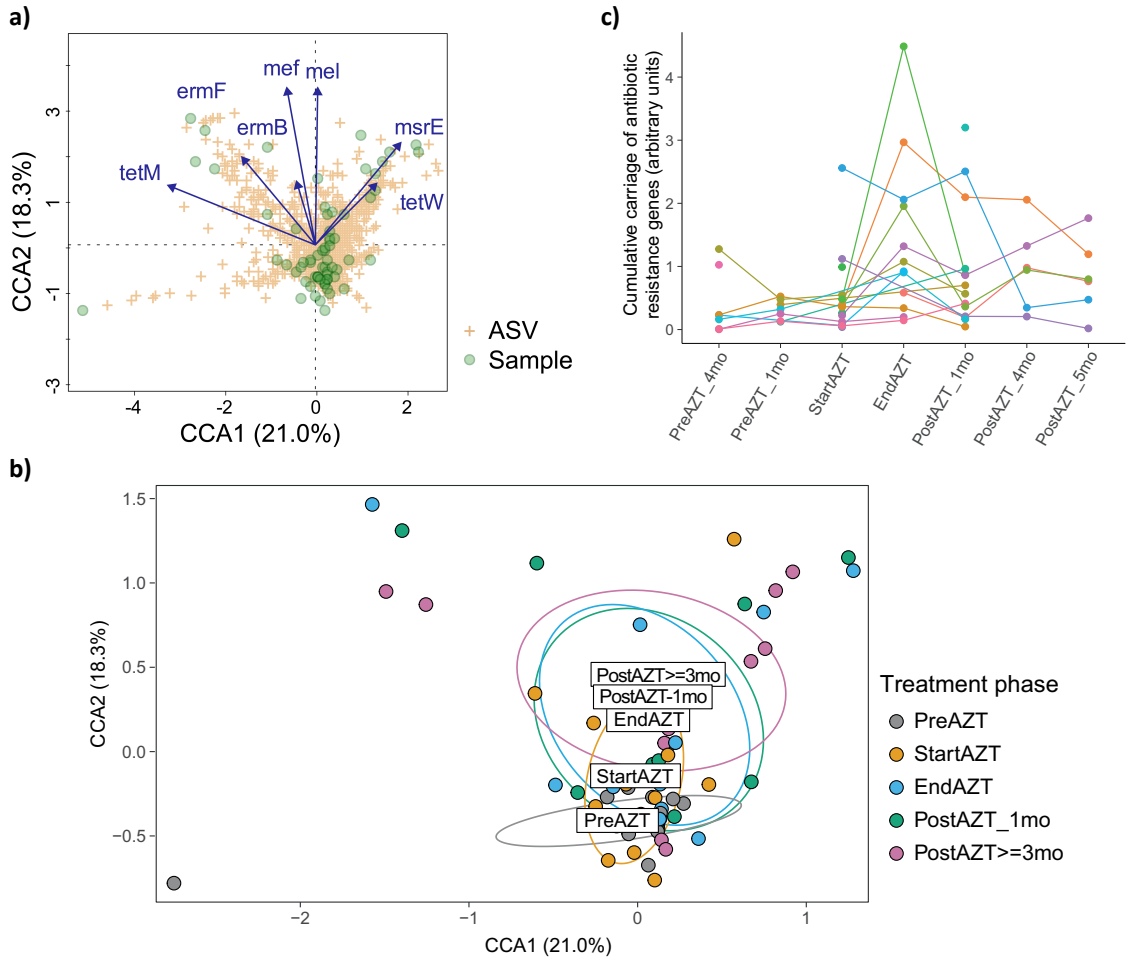

Figure 5. Acquisition of ARG during AZT treatment in LRT. (*a* and *b*) Canonical correlation analysis showing that ARG carriage was limited to a minority of sputum samples (circles) and ASVs (crosses) (*a*), and stratification by treatment phase showing that almost all samples with ARG were taken at the end of AZT treatment or later (*b*). (*c*) Within-patient monitoring of the cumulative sum of normalised copy numbers of the full set of ARG genes, focusing on patients with more than one sputum sample available, showing the increase in ARG carriage after the start of AZT treatment.

Abbreviations: ARG = antibiotic resistance genes; AZT = azithromycin; LRT = lower respiratory tract; ASVs = amplicon sequence variants

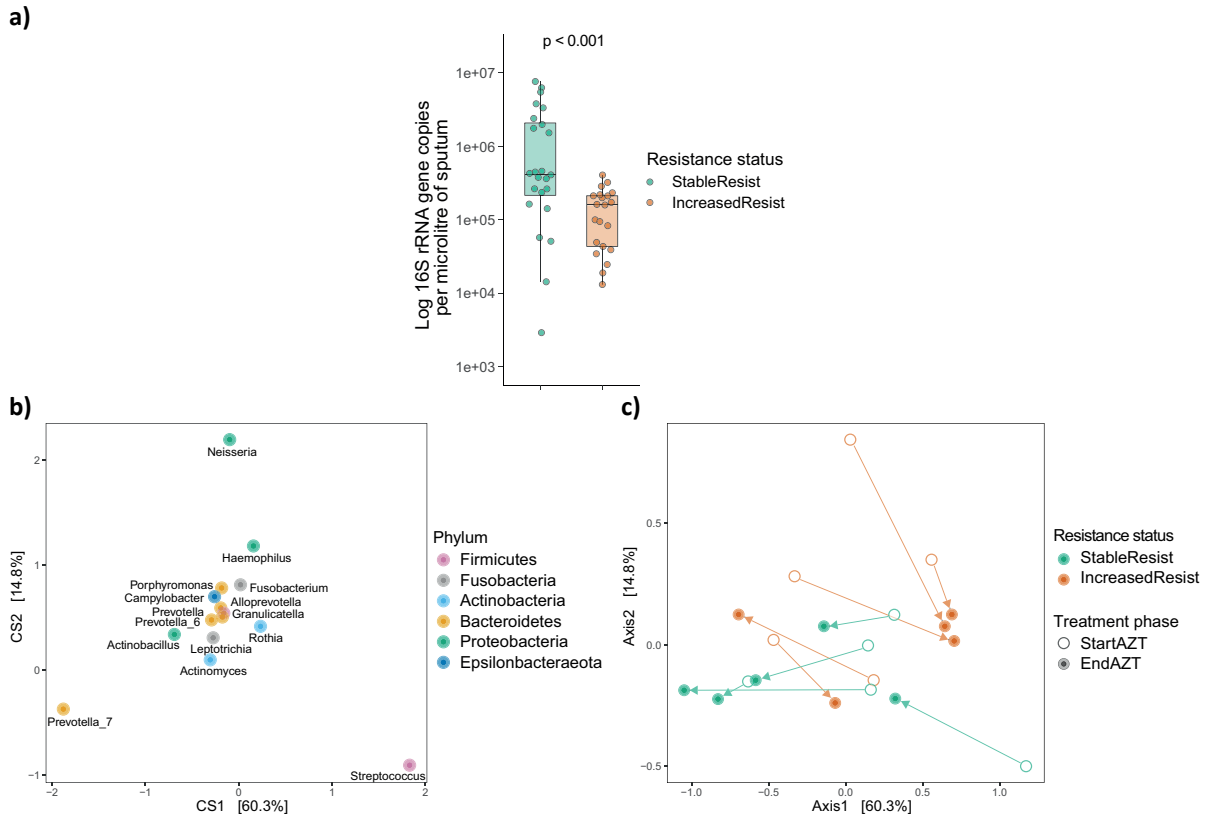

Figure 6. Relationship between the difference in ARG carriage during AZT treatment, bacterial density and the 15 dominant genera of the LRT microbiota. (*a*) qPCR determination of bacterial density showing lower levels in patients with increased resistance. Middle lines, boxes and whiskers represent the median, interquartile range (IQR) and 1.5 times the IQR, respectively. Dots represent samples. Kruskal-Wallis with Dunn's post hoc test. (*b* and *c*) Double PCoA showing the influence of *Prevotella_7* abundance in the compositional changes occurring during AZT treatment in patients with stable resistance, respectively *Streptococcus* abundance in patients with increased resistance. In panels *b* and *c*, dots represent different phyla and samples, respectively. In panel *c*, the arrows link LRT samples collected from a single patient at the start and end of AZT treatment.
Abbreviations: ARG = antibiotic resistance genes; AZT = azithromycin; LRT = lower respiratory tract; qPCR = quantitative polymerase chain reaction; PCoA = principal coordinate analysis

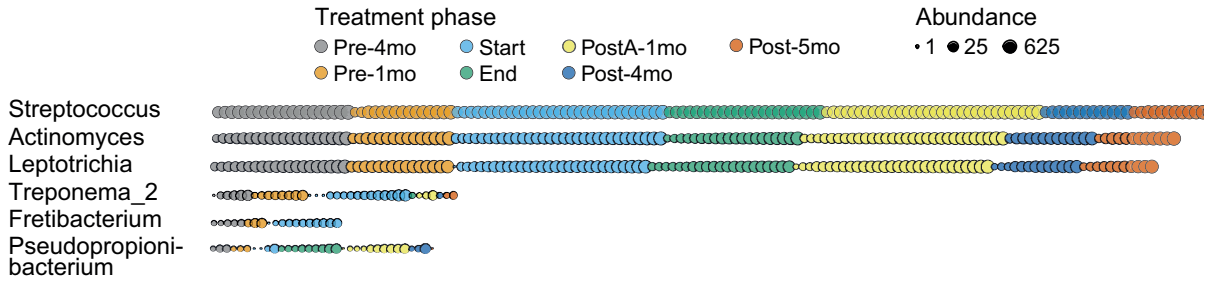

Figure 7. Genera most affected by loss and/or acquisition of ASVs in LRT during AZT treatment. Dot plot showing the prevalence (number of dots each representing a sample) and abundance (dot size in log scale) of selected genera during the study phases (colour code). *Streptococcus*, *Actinomyces* and *Leptotrichia* illustrate genera whose abundance and prevalence prior to treatment, and partial replacement during treatment, allowed maintenance throughout the study. *Treponema_2* and *Fretibacterium* on one side, and *Pseudopropionibacterium* on the other, illustrate a decrease, respectively a transient increase in prevalence linked to treatment.
Abbreviations: LRT = lower respiratory tract; AZT = azithromycin; ASVs = amplicon sequence variants

Azithromycin alters spatial and temporal dynamics of airway microbiota in idiopathic pulmonary fibrosis

Authors:

*Pieter-Jan Gijs[a], *Cécile Daccord[a], Eric Bernasconi[a], Martin Brutsche[b], Christian Clarenbach[c], Katrin Hostettler[d], Sabina A. Guler[e], Louis Mercier[a], Niki Ubags[a], +Manuela Funke-Chambour[e] and +Christophe von Garnier[a]

Affiliations

[a] Division of Pulmonology, Department of Medicine, CHUV, Lausanne University Hospital, Lausanne, University of Lausanne, Switzerland
[b] Lung center, Kantonsspital St. Gallen, St. Gallen, Switzerland
[c] Division of Pulmonary Medicine, University Hospital of Zurich, Zurich, Switzerland
[d] Clinics of Respiratory Medicine, University Hospital Basel, Basel, Switzerland
[e] Department of Pulmonary Medicine, Inselspital, Bern University Hospital, Bern, Switzerland

* Shared first authorship
+ Shared last authorship

Corresponding Author:

Niki Ubags
Division of Pulmonology, Department of Medicine, CHUV, Lausanne University Hospital, Lausanne, University of Lausanne, Switzerland
Email : Niki.Ubags@chuv.ch

Supplementary materials and methods

Study population and sample collection

The study was conducted between August 2014 and August 2019; Key inclusion criteria were age over 18 years and a diagnosis of IPF according to current diagnostic guidelines(1). Ethical approval was obtained prior to the start of the study (KEK 002/14), and all patients provided written consent prior to inclusion in the study.

Patients with one or more of the following criteria were excluded: any change in medication or respiratory infection within four weeks prior to inclusion, known allergy or intolerance to macrolide antibiotics, known cardiac arrhythmia, severe renal failure, history of hepatitis, current alcohol or drug abuse, serum bilirubin level of > 50 µmol/L, elevated aspartate transaminase or alanine transaminase by more than three times the upper limit of normal, or QTc prolongation on 12-lead electrocardiogram.

Oropharyngeal swab (OPS) and sputum samples were collected at different time points of the study for characterisation of the microbiota of the upper respiratory tract (URT) and lower respiratory tract (LRT), respectively (**Supplementary Figure E1**). When sputum could not be produced it was induced by inhalation of a 3% sodium chloride solution (details not available if sputum were spontaneous or induced). Samples were frozen at -80°C at each collection centre and then transferred to Lausanne University Hospital for DNA extraction and sequencing.

Bacterial DNA extraction

The reducing agent dithiothreitol (DTT [AppliChem, Darmstad, Germany], final concentration up to 5% for 15 min at room temperature) was used to homogenise the mucus phase of thawed sputum samples. Bacterial DNA from sputum and OPS samples was then extracted using the DNeasy UltraClean microbial kit (Qiagen, Hilden, Germany), modified by pre-incubating with 9000 U Ready-Lyse lysozyme (Epicentre, Hessisch Oldendorf, Germany) for 1 hour at 37°C. Purified DNA was eluted in 30 µl of microbial DNA-free water (Qiagen).

16S rRNA amplicon quantification

The copy numbers of the 16S rRNA gene were determined by qPCR using previously reported primers specific to pan bacteria(2) (see Supplementary Table E00). Amplification was performed using SsoAdvanced Universal SYBR Green Supermix (Bio-Rad, Hercules, CA) on a CFX96 Real-Time detection system (Bio-Rad) with the following cycling parameters: initial 2 min denaturation at 98 °C, followed by 45 cycles of 5 s denaturation at 98 °C, and 60 s annealing/elongation at 61.5 °C. Absolute quantification was performed based on a standard curve obtained with a purified amplicon product.

16S rRNA amplicon sequencing

Bacterial community composition was assessed by Illumina MiSeq sequencing with barcoded primers targeting the V1-V2 region (**Supplementary Table E1**). Amplification was performed using the Accuprime Taq DNA Polymerase High Fidelity kit (Invitrogen, Waltham, MA). Duplicate PCR reactions of 20 µl consisted of 2 µl of 10× Accuprime buffer II, 0.44 µl of each 10 mM barcoded primer F-27 and R-338, 9.03 µl of ultrapure water, 0.09 µl of AccuPrime Taq DNA Polymerase and 8 µl of DNA template with the following cycling parameters: initial 3 min denaturation at 94 °C, followed by 40 cycles of 30 s denaturation at 94 °C, 30 s annealing at 56 °C and 90 s elongation at 72 °C, with a final extension at 72 °C for 5 min. No-template PCR reaction controls (n = 2) were included. Amplicons were quantified using a LabChip GX instrument with the DNA 1 K kit (Perkin Elmer, Waltham, MA), pooled into equimolar amounts and purified using the AMPure XP bead cleaning system (Beckman Coulter, Brea, CA). Libraries were then diluted to 12 pM and spiked with 25% phiX before being loaded onto the Illumina MiSeq platform using pairwise chemistry, generating 250 × 2 read lengths.

Analysis of antibiotic resistance gene carriage

Quantification of carriage of antibiotic resistance genes (ARG) targeting 23S ribosomal RNA methyltransferases (*erm*(B) and *erm*(F)), ATP-binding cassette ribosomal protection protein (*mel* and *msr*[E]), major facilitator superfamily antibiotic efflux pump (*mef*), and tetracycline-resistant ribosomal protection proteins (*tet*[M] and *tet*[W]) was performed on sputum specimens using dye-based (SsoAdvanced Universal SYBR Green, Bio-Rad) or probe-based real-time PCR assays, using primer pairs, probes and conditions previously described(3). To accommodate the limited material available for OPS samples, only *mel* and *tet*(W) gene expression was quantified, using the same qPCR protocol. Absolute quantification was performed based on standard curves obtained with purified amplicon products. The absolute copy number of resistance genes per sample was

normalised to the 16S rRNA gene copy number used as a proxy for bacterial number. To obtain a synthetic picture of ARG carriage per sample, the absolute counts obtained for each individual gene were scaled from 0 to 1 to give equal importance to each gene, and the cumulative counts were reported.

Bioinformatics and statistical analysis

All analyses were performed in R version 4.1.0. Bioinformatics processing, which included demultiplexing, removal of chimeric and short reads, single-base resolution of reads into amplicon sequence variants (ASVs) using the Divisive Amplicon Denoising Algorithm 2 (DADA2) algorithm(4) and taxonomic annotation using the SILVA database(5), was performed using a dedicated pipeline available at https://github.com/chuvpne/dada2-pipeline. Initial abundance filtering of absolute read counts (threshold > 1) was applied in phyloseq 1.38.0, reducing the total number of ASVs detected in all OPS and sputum samples, as well as in controls, from 4,233 to 4,170. Filtering based on ASVs belonging to the Bacteria kingdom further reduced the total number of ASVs from 4,170 to 4,099. We filtered potential contaminants using two complementary methods within decontam 1.14.0 R package(6). The prevalence method, based on the prevalence of ASVs in negative controls versus patient samples, identified 84 contaminants and 4015 non-contaminants (**Supplementary Figure E2a** and **Table E2**). The frequency method is based on the relationship between the relative abundance of ASVs and bacterial density, with the assumption that a negative correlation is characteristic of contaminants. This approach identified 50 contaminants and 4049 non-contaminants (**Supplementary Figure E2b** and **Table E3**). ASV26_Pseudomonas was the only ASV considered as a contaminant by both methods. ASV26_Pseudomonas and ASV6_Cutibacterium showed the strongest contaminant signature (**Supplementary Figure E2a**), as further confirmed by rank analysis of the 15 most abundant ASVs in control samples versus patient samples (**Supplementary Figure E7**). This combined screening identified 133 different ASVs as contaminants that we excluded for downstream analysis.

In addition, 12 OPS samples were excluded based on a sequencing depth not exceeding that in the majority of controls (**Supplementary Figure E5**), despite a bacterial density not similarly low (**Supplementary Figure E4**). Specifically, examination of the sequencing depth per sample (median 3.5×10^4, interquartile range 1.7×10^4 to 5.4×10^4) showed that above the threshold of 10^4, there were 1.4% controls (2 controls, 77 oropharyngeal swabs, 67 sputum samples), whereas below this threshold, the proportion of controls rose to 47.8% (11 controls, 12 oropharyngeal swabs. This latter filtering removed 210 ASVs.

Finally, we performed rarefaction on the remaining 3,756 samples, using the “rarefy_even_depth” command from phyloseq 1.38.0, which set the threshold of reads to 10,055 per sample, and removed ASVs, leaving a total of 3,483 ASVs in 146 samples (**Supplementary Figure E3**).

In downstream analyses, the relative abundance of each ASV was Hellinger transformed(7) using the "decostand" function in vegan 2.6-2. The different alpha diversity measurements were performed using the alpha function in Microbiome 1.16.0. Principal coordinate analysis (PCoA) was used to visualise beta diversity based on unweighted UniFrac distance in vegan 2.6-2 and ggordiplots 0.4.1. Canonical correlation analysis (CCA) was performed using the cca function in vegan 2.6-2 to show the link between variation in respiratory microbiota composition and AR gene carriage. To compare changes in respiratory microbiota between the start and end of AZT treatment in patients with stable vs. increased ARG carriage, we performed a double PCoA, which combines analysis of phylogenetic and abundance data. To this end, we agglomerated the dataset at genus level, retained the 15 most abundant genera, and constructed a phylogenetic tree using the rtree function in ape 5.6-2. DPCoA was then performed using the ordinate function in phyloseq 1.38.0. All analyses were performed in R version 4.1.0.

R scripts are available at https://github.com/CHUVpulmonology/Airway_microbiota-Lung_fibrosis-Azithromycin. The original sequencing data and the starting data for the analyses in R are available at 10.5281/zenodo.7065053.

References

1. Raghu, G, Remy-Jardin M, Myers JL *et al.* Diagnosis of Idiopathic Pulmonary Fibrosis An Official ATS/ERS/JRS/ALAT Clinical Practice Guideline. *Am J Respir Crit Care Med* **198**, 44–68 (2018).
2. Bacchetti De Gregoris T, Aldred N, Clare AS *et al.* Improvement of phylum- and class-specific primers for real-time PCR quantification of bacterial taxa. *J Microbiol Methods* **86**, 351–356 (2011).
3. Taylor SL, Leong LEX, Mobegi FM *et al.* Long-Term Azithromycin Reduces Haemophilus influenzae and Increases Antibiotic Resistance in Severe Asthma. Am J Respir Crit Care Med. **200(**3):309-317 (2019).
4. Callahan BJ, McMurdie PJ, Rosen MJ *et al.* DADA2: High-resolution sample inference from Illumina amplicon data. *Nature Methods 2016 13:7* **13**, 581–583 (2016).
5. Quast C, Pruesse E, Yilmaz P *et al.* The SILVA ribosomal RNA gene database project: improved data processing and web-based tools. *Nucleic Acids Research* **41**, D590 (2013).
6. Davis, NM, Proctor DM, Holmes SP *et al*. Simple statistical identification and removal of contaminant sequences in marker-gene and metagenomics data. *Microbiome* **6**, 1–14 (2018).
7. Legendre P, Gallagher ED. Ecologically meaningful transformations for ordination of species data. *Oecologia* **129**, 271–280 (2001).

Supplementary Figures

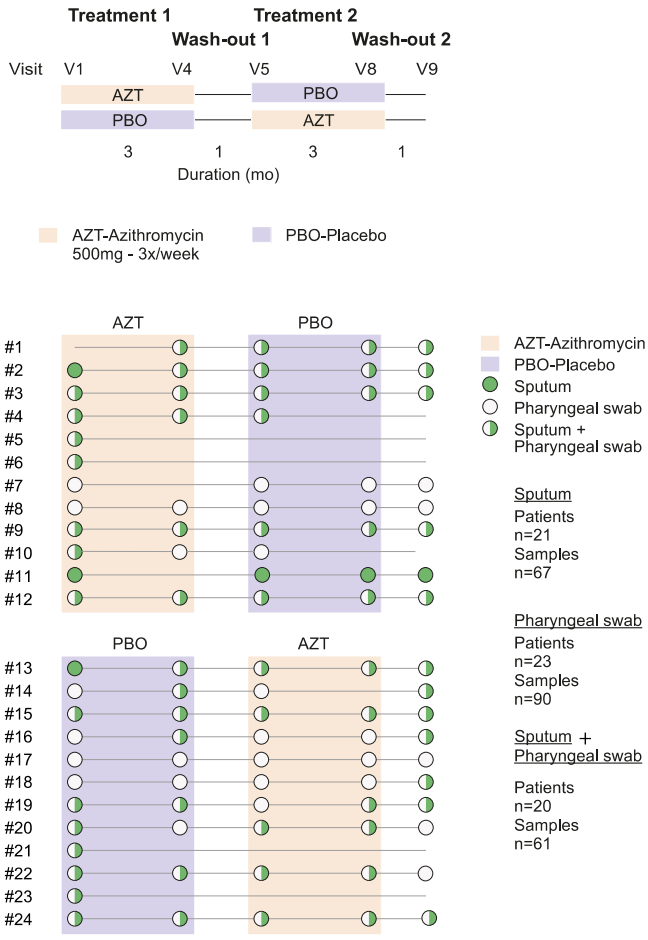

Supplementary Figure E1. Study design and grid of colour-coded collected specimens

a)

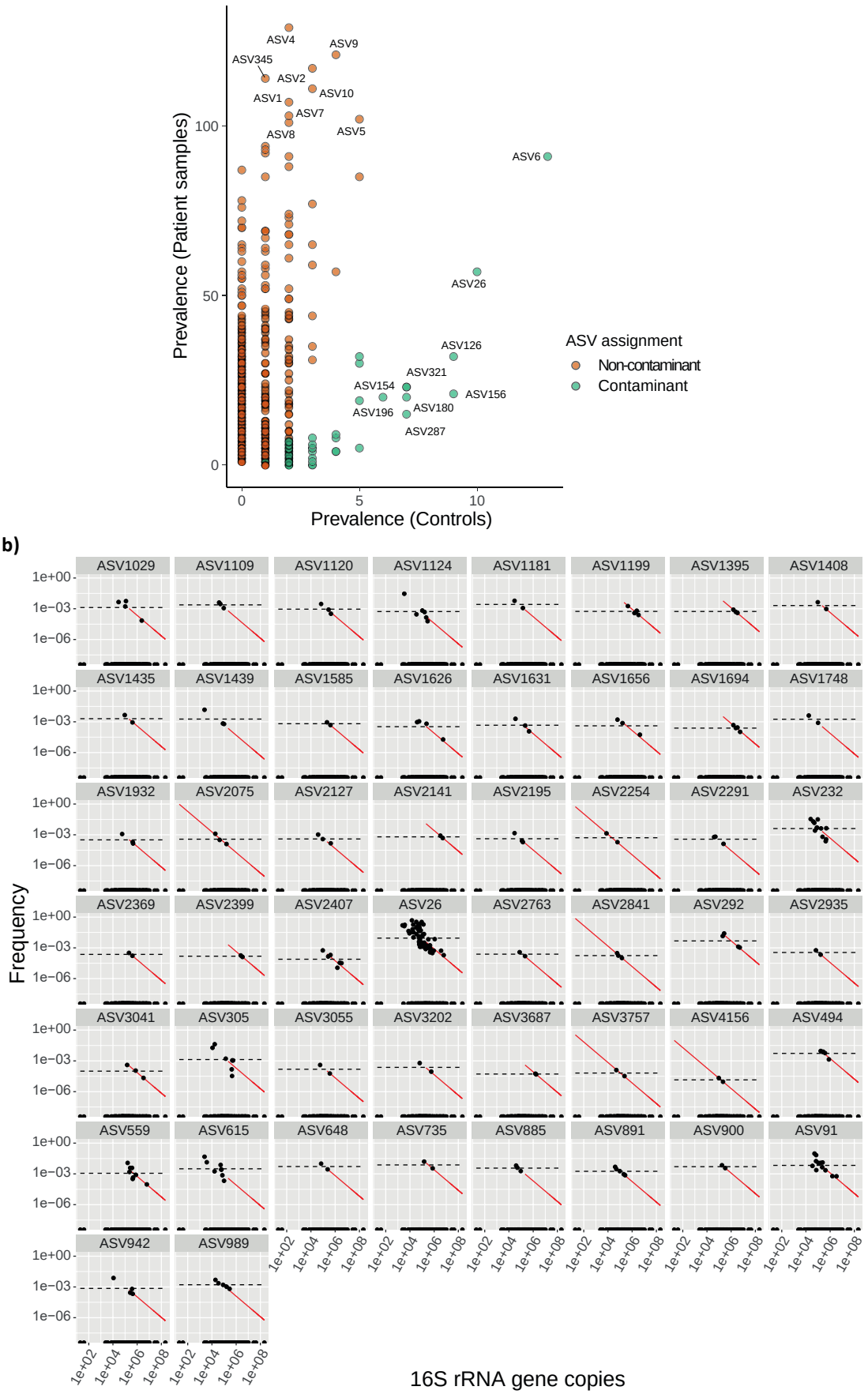

Supplementary Figure E2. Contaminant screening. Contaminants were identified using decontam R package combining the prevalence method based on the prevalence of ASVs in color-coded negative controls versus patient samples (a) and the frequency method based on the relationship between the relative abundance of ASVs (frequency, y-axis) and bacterial density (16S rRNA gene copies, x-axis) (b). The prevalence method and the frequency method identified 50 and 84 contaminants, respectively (see Tables E2 and E3 for the names of the

taxa with the strongest contaminant signatures), with only one ASV (ASV26 - *Pseudomonas* sp.) considered a contaminant in both methods, leading to the filtering out of a total of 133 contaminants.
Abbreviations: ASVs = amplicon sequence variants

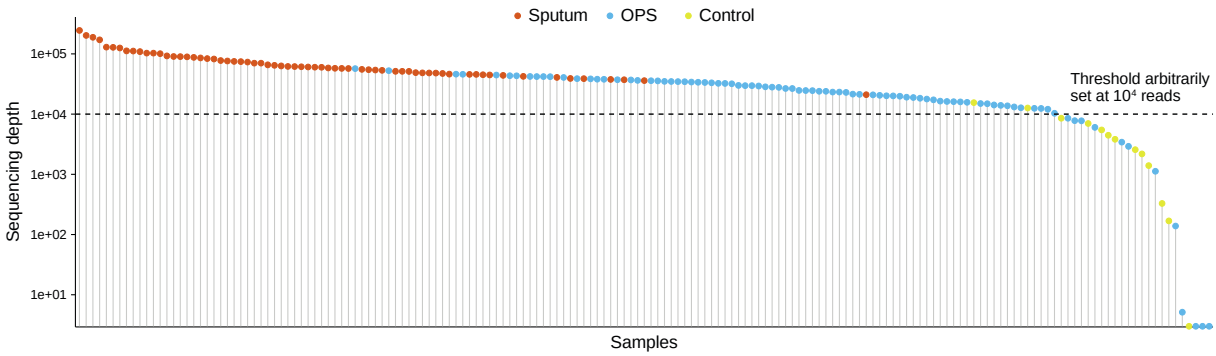

Supplementary Figure E3. Number of reads for each sputum, OPS and control sample. The threshold was arbitrarily set at 1.1 x 10^4 reads. 10 OPS samples were excluded for further analysis.
Abbreviations: OPS = oropharyngeal swab

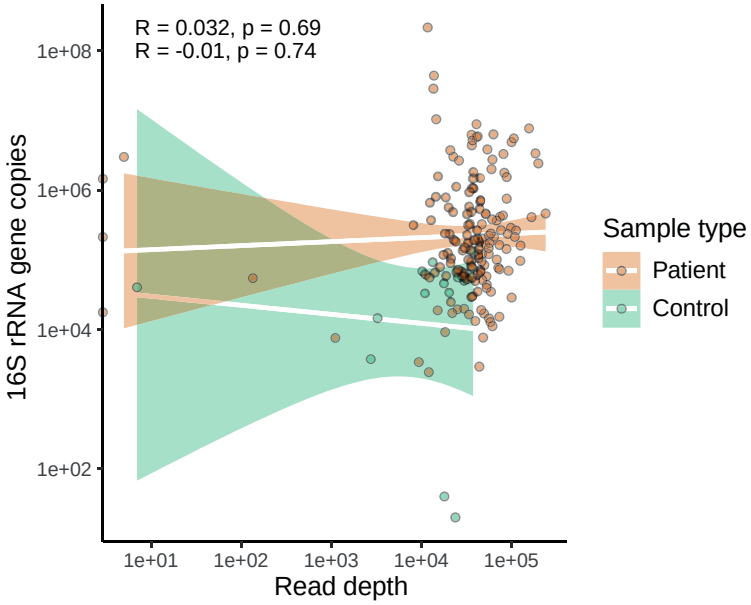

Supplementary Figure E4. Dot plot showing lack of correlation between bacterial density (y-axis) and read depth (x-axis) for patient samples and controls (color coded). Linear models with regression lines and R-squared values and p-values

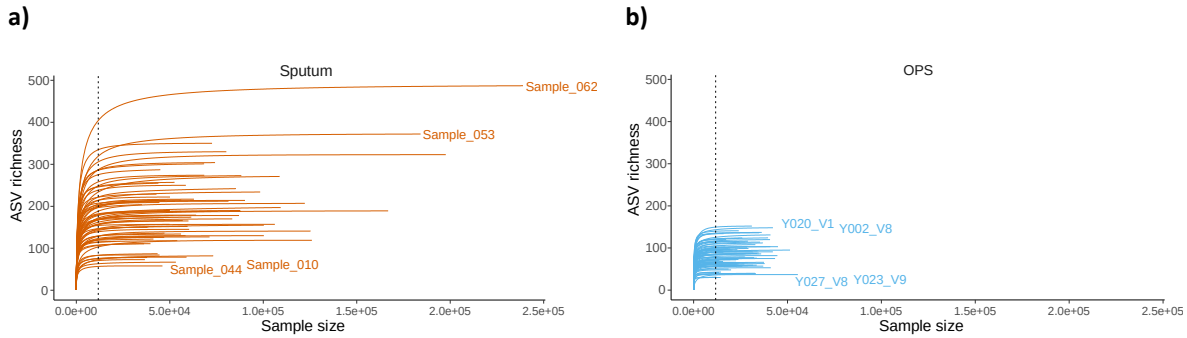

Supplementary Figure E5. Rarefaction curves obtained after abundance-based filtering and contaminant filtering for sputum (*A*) and OPS (*B*) samples, with indication of the 10,055 read depth used in downstream analyses (dashed line).
Abbreviations: OPS = oropharyngeal swab

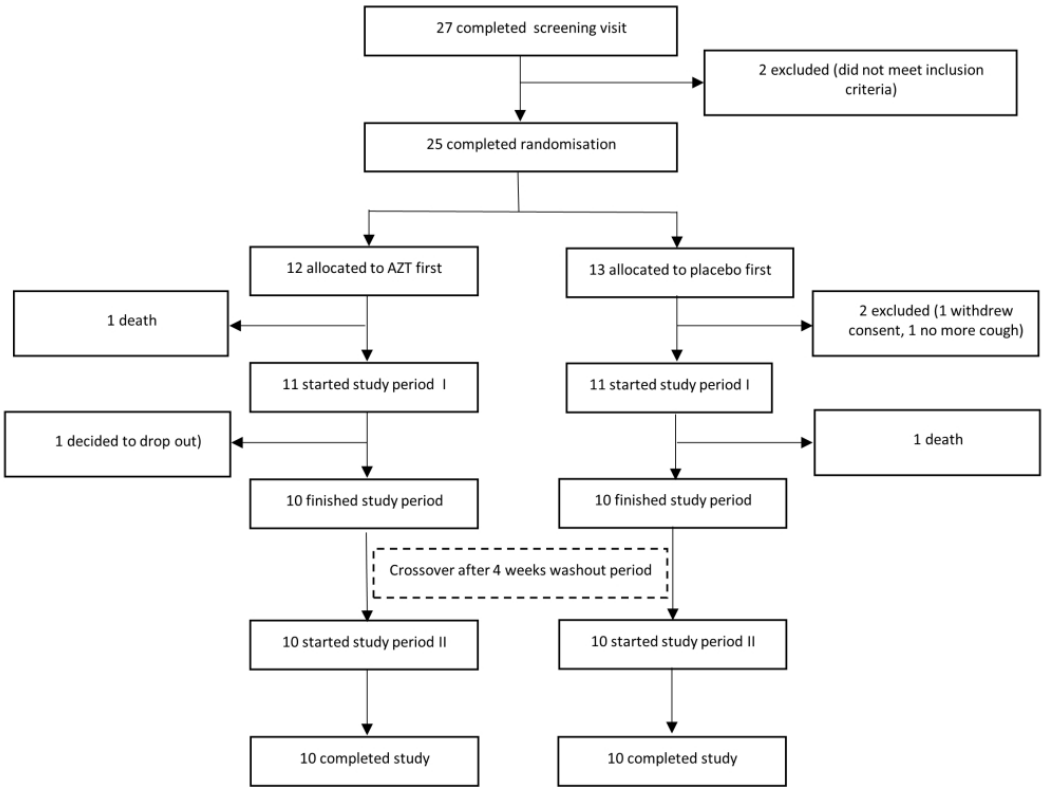

Supplementary Figure E6. CONSORT flow diagram of patients screening, inclusion, and analysis. The "*Azithromycin for the Treatment of Chronic Cough in Idiopathic Pulmonary Fibrosis*" was a prospective, randomized controlled crossover trial, of which the current study is a sub-analysis.

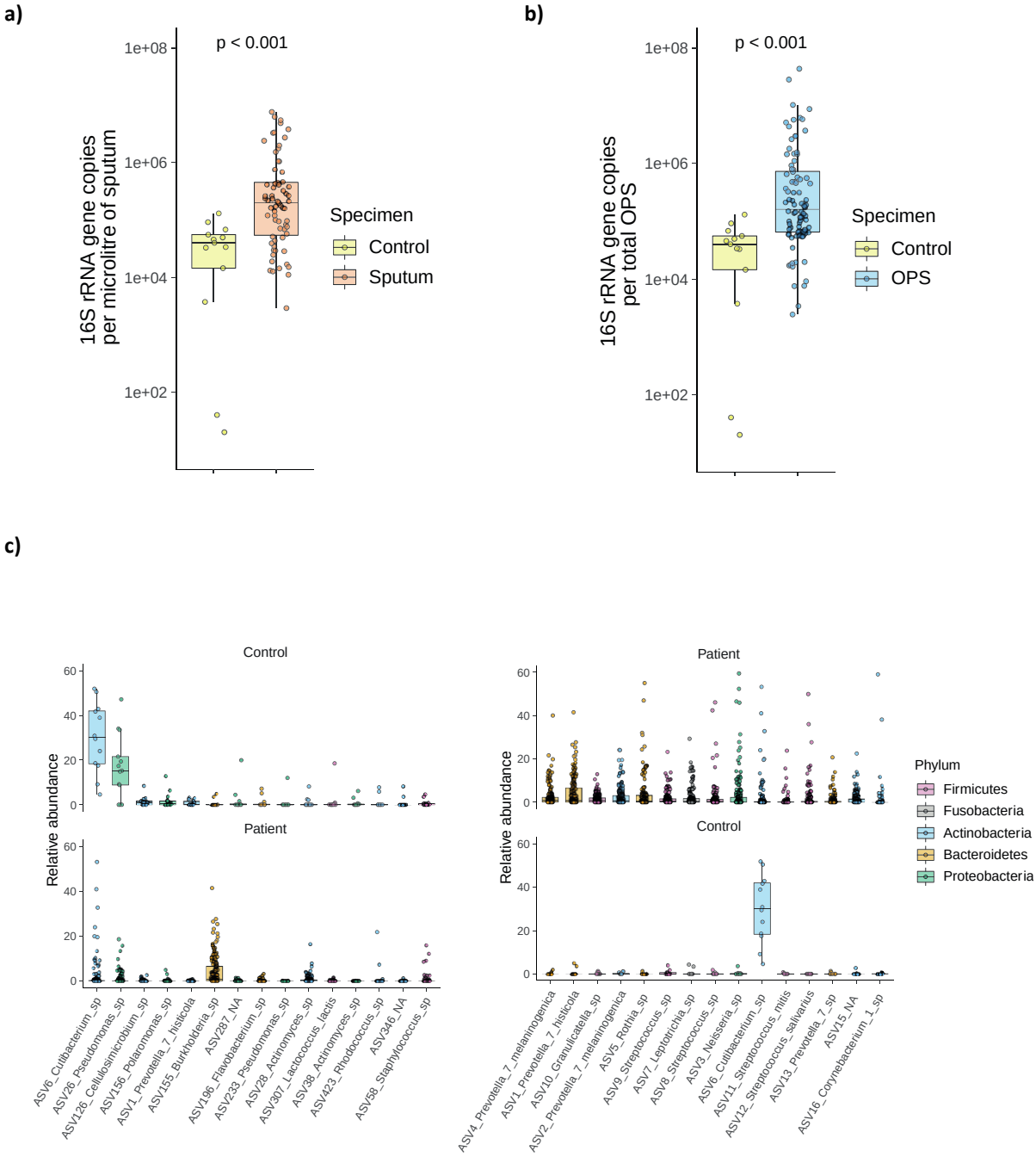

Supplementary Figure E7. Evidence of a distinct bacterial signal between patient samples and negative procedural controls. (*a* and *b*) The bacterial density in sputum (*a*) and OPS (*b*) samples from patients was significantly greater (p<0.001, Wilcoxon rank sum test) than that in negative controls. (*c*) Rank abundance comparison of prominent taxa detected in negative control (left) and patient (sputum combined with OPS, right) samples. For each comparison, the 15 most abundant taxa in each group are displayed in decreasing order of median relative abundance. In all box plots, the middle line, box and whiskers represent the median, interquartile range (IQR) and 1.5 times the IQR, respectively. Dots represent samples.

Abbreviations: OPS = oropharyngeal swab

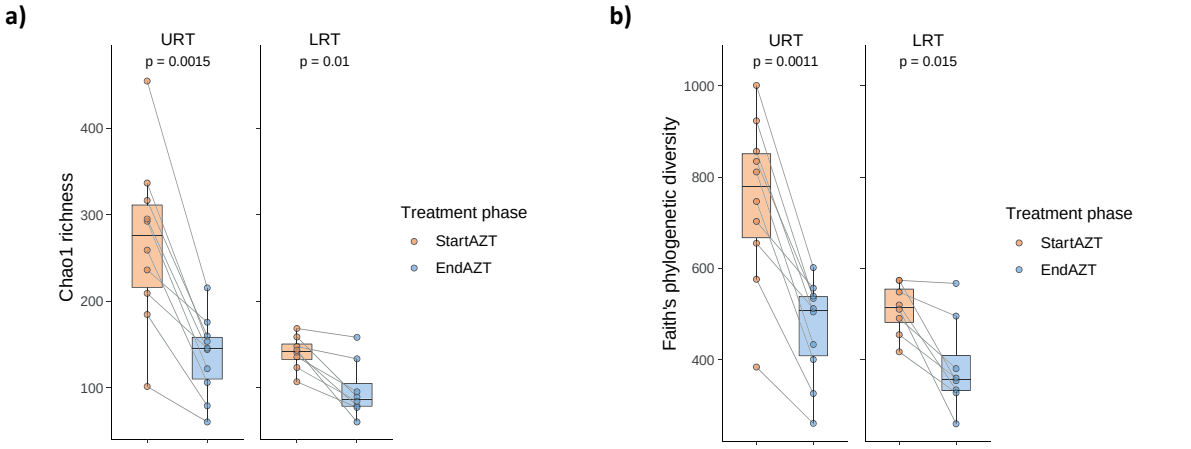

Supplementary Figure E8. Decrease in alpha diversity after AZT treatment. Intra-individual analyses showing a decrease in Chao1 richness (*a*) and Faith's phylogenetic diversity (*b*) in each of the 10 patients for whom sputum sample pairs were available and in each of the 8 patients for whom OPS pairs were available. Middle lines, boxes and whiskers represent the median, interquartile range (IQR) and 1.5 times the IQR, respectively. Dots represent samples and samples from a single patient are paired by a line. Wilcoxon signed-rank test.
Abbreviations: LRT = lower respiratory tract; URT = upper respiratory tract; AZT = azithromycin; OPS = oropharyngeal swab

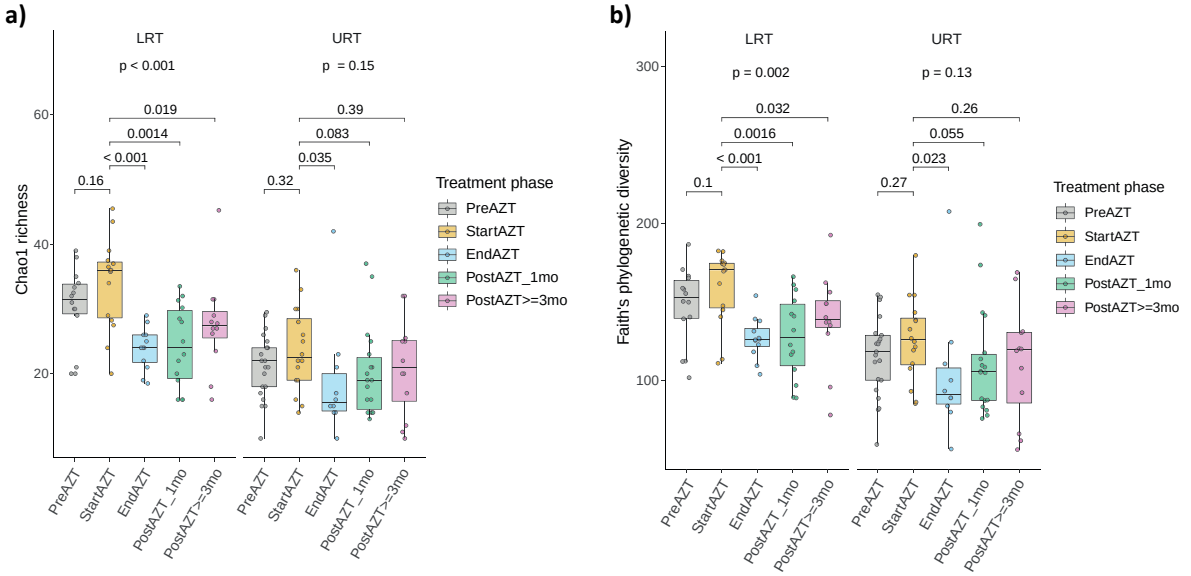

Supplementary Figure E9. Decrease in alpha diversity after AZT treatment, assessed at the genus level. (*a* and *d*) Alpha diversity metrics showing a decrease in Chao1 richness (*a*) and Faith's diversity (*b*) during AZT treatment in LRT and URT. Middle lines, boxes and whiskers represent the median, interquartile range (IQR) and 1.5 times the IQR, respectively. Dots represent samples. Kruskal-Wallis with Dunn's post hoc test.
Abbreviations: AZT = azithromycin; LRT = lower respiratory tract; URT = upper respiratory tract

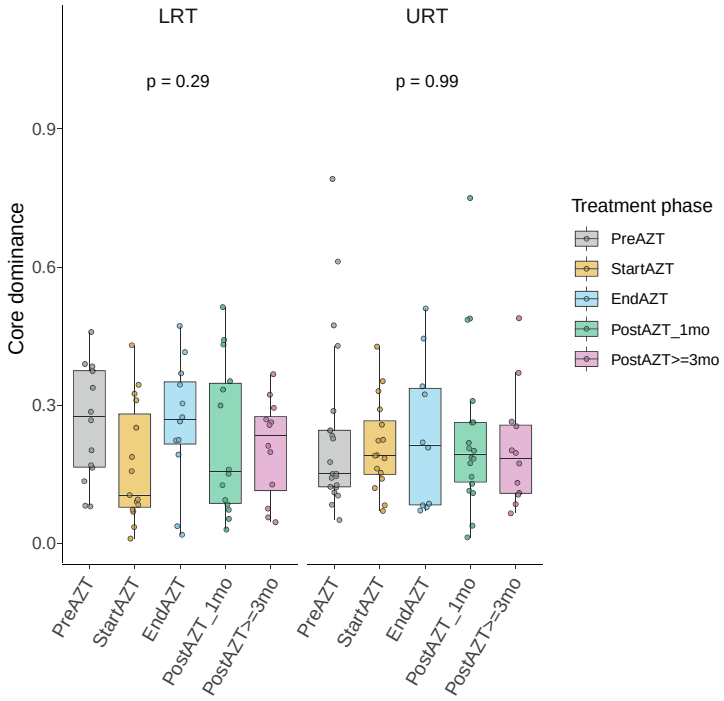

Supplementary Figure E10. Analysis of the dominance of the core community (species exceeding 0.2% relative abundance in more than 50% of the samples) showing no significant difference between the start and end of treatment in LRT or URT. Middle lines, boxes and whiskers represent the median, interquartile range (IQR) and 1.5 times the IQR, respectively. Dots represent samples. Kruskal-Wallis test.
Abbreviations: AZT = azithromycin; LRT = lower respiratory tract; URT = upper respiratory tract

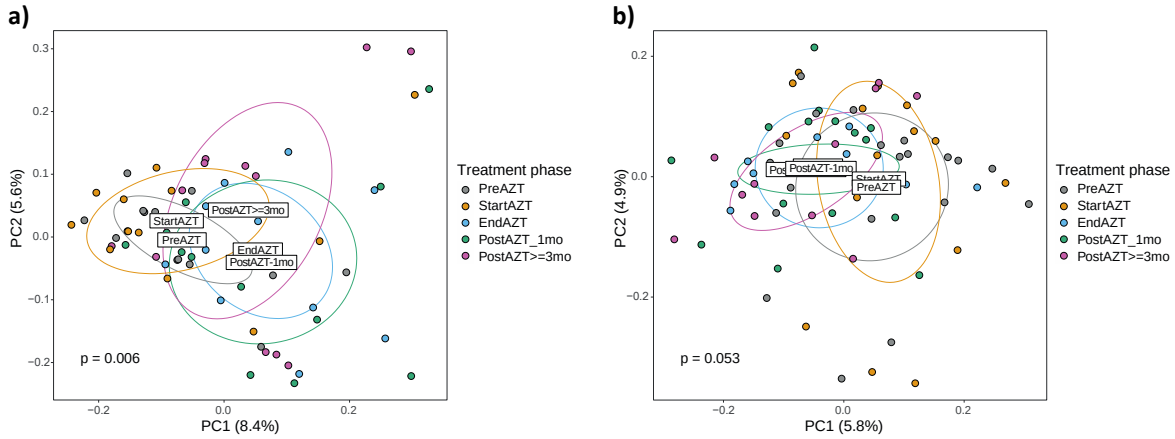

Supplementary Figure E11 (*a* and *b*) PCoA of bacterial communities based on unweighted UniFrac distance showing that the community composition of airway bacteria was distinct between specimens collected before or at the start of AZT treatment, compared to those collected at the end of treatment or later, in LRT (*a*). There was no significant difference in URT (*b*). In PCoA labels indicate the position of the centroid of the corresponding group, the label “EndAZT” is hidden by the label “PostAZT_1mo”. PERMANOVA.
Abbreviations: PCoA = principal coordinate analysis; AZT = azithromycin; LRT = lower respiratory tract; URT = upper respiratory tract

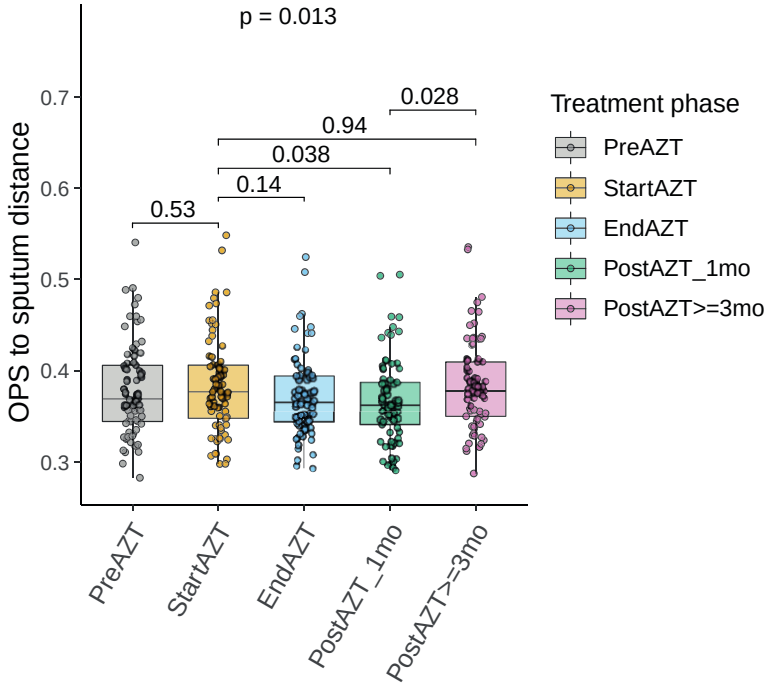

Supplementary Figure E12. AZT treatment transiently reduces dissimilarity between LRT and URT microbiota based on weighted UniFrac distance. For each treatment phase, weighted UniFrac distance was calculated between each OPS sample and the centroid obtained from the corresponding set of sputum samples. The weaker impact of AZT treatment on dissimilarity between LRT and URT microbiota when based on weighted UniFrac distance compared to unweighted UniFrac distance indicates that relatively low abundance taxa are mainly affected. Middle lines, boxes and whiskers represent the median, interquartile range (IQR) and 1.5 times the IQR, respectively. Dots represent samples. Kruskal-Wallis with Dunn's post hoc test.
Abbreviations: AZT = azithromycin; OPS = oropharyngeal swab; LRT = lower respiratory tract; URT = upper respiratory tract

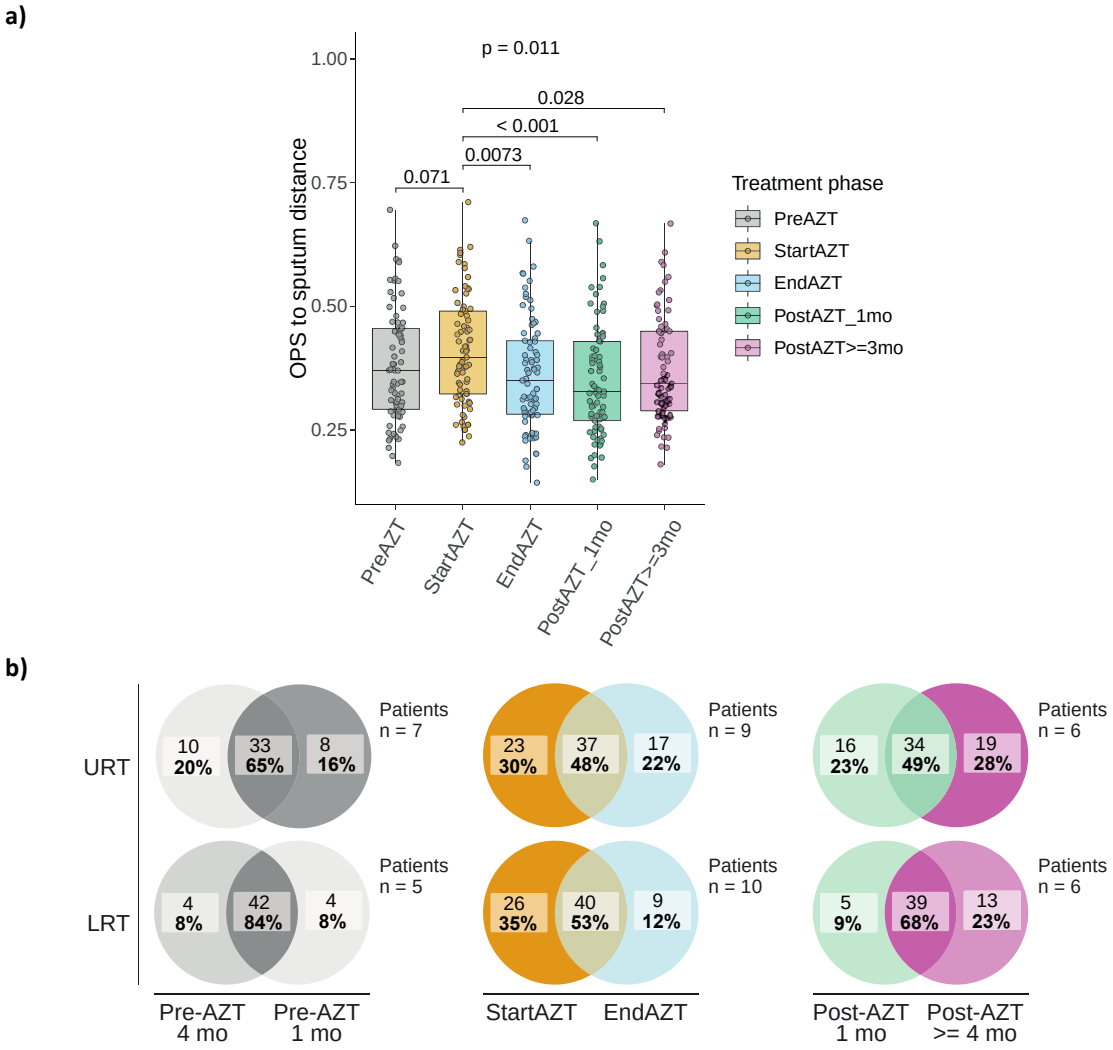

Supplementary Figure E13. AZT treatment reduces dissimilarity between LRT and URT microbiota at genus level. (*a*) Unweighted UniFrac distance calculated for each treatment phase between each OPS sample and the centroid obtained from the corresponding set of sputum samples. Middle lines, boxes and whiskers represent the median, interquartile range (IQR) and 1.5 times the IQR, respectively. Dots represent samples. Kruskal-Wallis with Dunn's post hoc test. (*b*) Venn diagrams of the total numbers and proportions of genera represented either at the start, at the end or retained over a 3-month time window, showing treatment-induced alterations in the temporal dynamics of the LRT and URT microbiota.

Abbreviations: AZT = azithromycin; LRT = lower respiratory tract; URT = upper respiratory tract; OPS = oropharyngeal swab

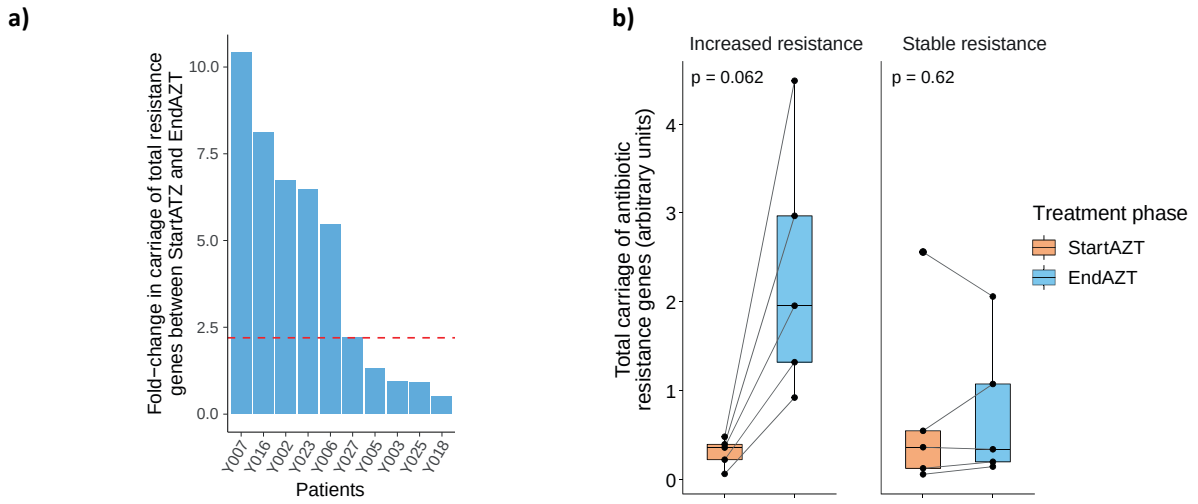

Supplementary Figure E14. Patient-specific fold-change in the cumulative sum of seven pooled ARG in the LRT during AZT treatment. (*a*) Separation into two groups of patients according to the median fold-change (3.8; red dotted line; ranges 5.5-10.4 and 0.51-2.2 for the groups of patients considered to have shown increased resistance, respectively stable resistance, during treatment). (*b*) Kinetics of ARG carriage in the two groups of patients with increased or stable resistance during AZT treatment. Middle lines, boxes and whiskers represent the median, interquartile range (IQR) and 1.5 times the IQR, respectively. Dots represent samples and samples from a single patient are paired by a line. Wilcoxon signed-rank test.
Abbreviations: ARG = antibiotic resistance genes; LRT = lower respiratory tract; AZT = azithromycin

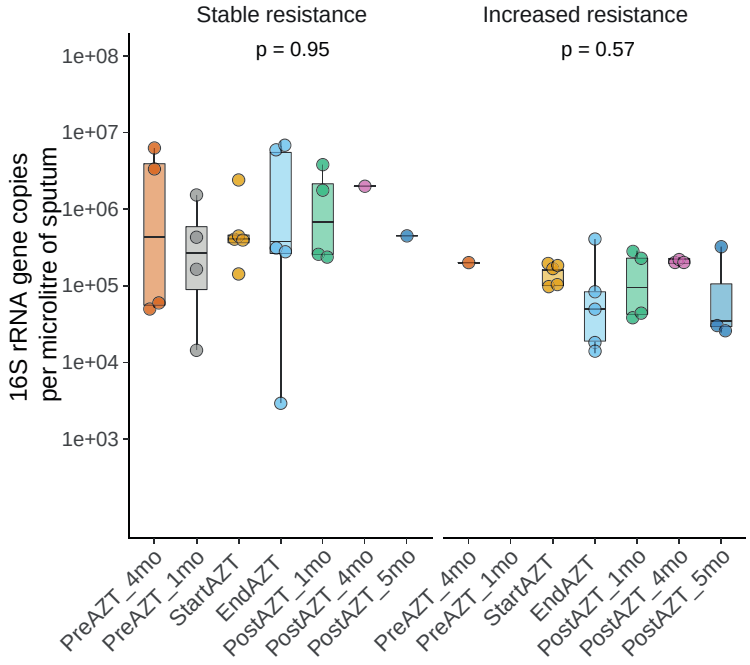

Supplementary Figure E15. Bacterial density evolution between treatment phases in LRT. There was no change in bacterial density between treatment phases, regardless of ARG carriage. Middle lines, boxes and whiskers represent the median, interquartile range (IQR) and 1.5 times the IQR, respectively. Dots represent samples. Kruskal-Wallis test.
Abbreviations: LRT = lower respiratory tract; ARG = antibiotic resistance genes

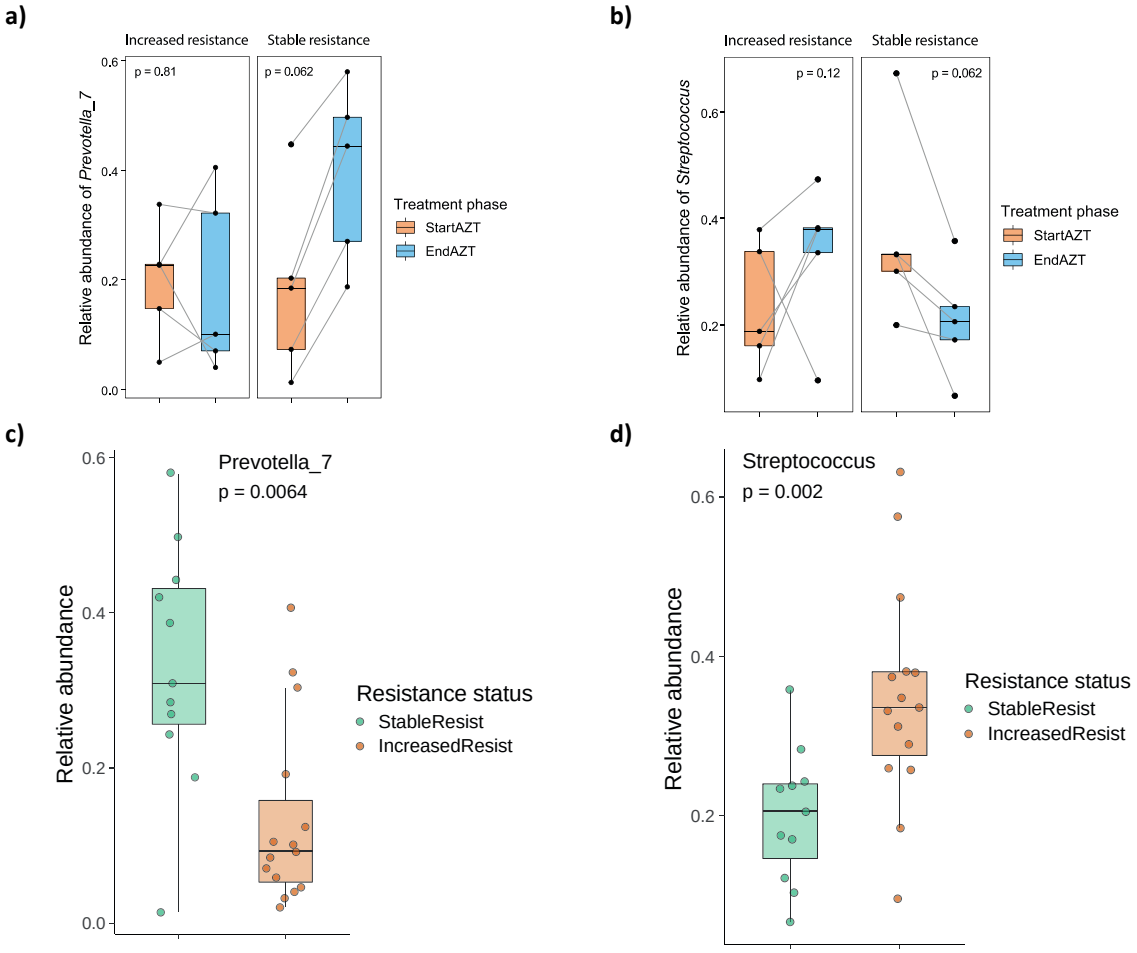

Supplementary Figure E16. Changes in the composition of the LRT microbiota in relation to ARG carriage during AZT treatment. (*a*) Increase in the relative abundance of the genus *Prevotella_7* in all five patients with stable ARG carriage and more disparate changes in patients with increased ARG carriage. (*b*) Decrease in the relative abundance of the genus *Streptococcus* in all five patients with stable ARG carriage and more disparate changes in patients with increased ARG carriage. (*c*) Relative abundance of *Prevotella_7* showing higher levels in patients with stable resistance. (*d*) Relative abundance of *Streptococcus* showing higher levels in patients with increased resistance. Middle lines, boxes and whiskers represent the median, interquartile range (IQR) and 1.5 times the IQR, respectively. Dots represent samples. Samples from a single patient are paired by a line. Significance tested using Wilcoxon signed-rank test (*a* and *b*) or Wilcoxon rank sum test (*c* and *d*).
Abbreviations: LRT = lower respiratory tract; ARG = antibiotic resistance genes; AZT = azithromycin

a)

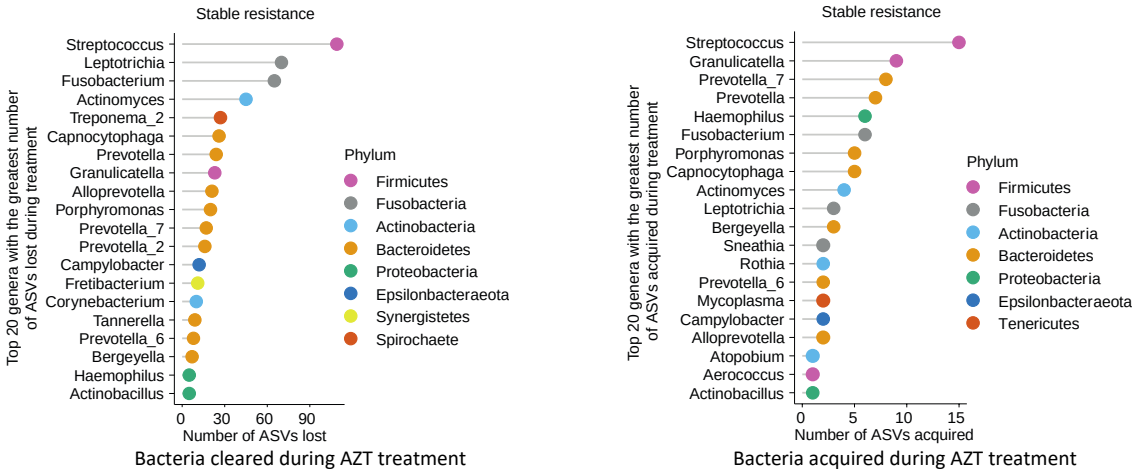

b)

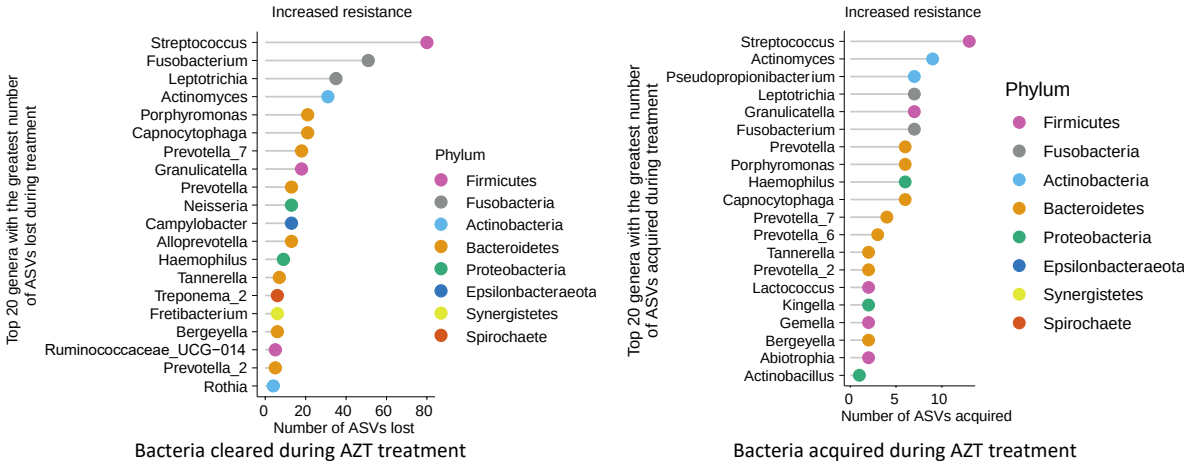

Supplementary figure E17. Genera most affected by loss and/or acquisition of ASVs in sputum during AZT treatment. (*a* and *b*) Lollipop chart showing for patients with stable (a) or increased (b) ARG carriage the number of ASVs lost (left panels) or acquired (right panels) during treatment, classified by genus. Regardless of resistance status, *Streptococcus*, *Leptotrichia*, *Fusobacterium* and *Actinomyces* were the genera with the highest number of ASVs lost during treatment and were also represented among the lower numbers of ASVs acquired during treatment, suggesting partial replacement

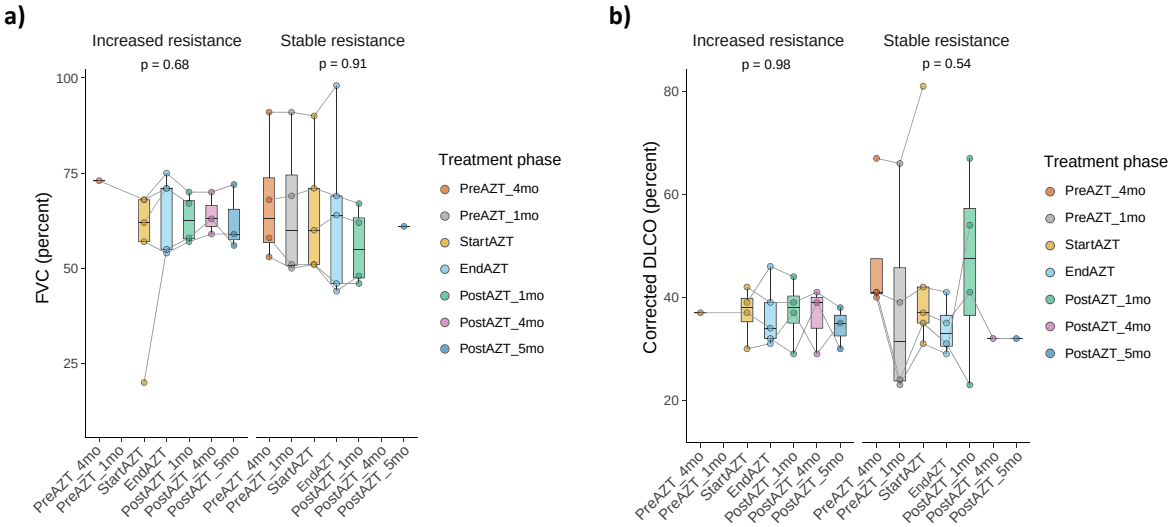

Supplementary Figure E18. Links between AZT treatment-related carriage of ARG in the LRT microbiota and lung function curves. (*a* and *b*) Analysis of LRT samples from patients with available ARG carriage status (n = 10) showing no consistent variations between patients in FVC (*a*) and DLCOc (*b*) during the different phases of treatment, independently of AR gene carriage. Middle lines, boxes and whiskers represent the median, interquartile range (IQR) and 1.5 times the IQR, respectively. Dots represent samples and samples from a single patient are paired by a line. Kruskal-Wallis test.
Abbreviations: AZT = azithromycin; ARG = antibiotic resistance genes; LRT = lower respiratory tract; FVC = forced vital capacity; DLCOc = corrected diffusing capacity of the lung for carbon monoxide

Supplementary Tables

Table E1. Oligonucleotide primers for 16S ribosomal RNA gene analysis.

Name	Method	Sequence (5'-3')
27F	Illumina MiSeq	**AATGATACGGCGACCACCGAGATCTACAC***TATGGTAATTCC*AGMGTTYGATYMTGGCTCAG
338R	Illumina MiSeq	**CAAGCAGAAGACGGCATACGAGAT**NNNNNNNNNNNN*AGTCAGTCAGAA*GCTGCCTCCCGTAGGAGT
926F	qPCR	AAACTCAAAKGAATTGACGG
1062R	qPCR	CTCACRRCACGAGCTGAC

Note: 27F and 338R Illumina sequencing primers allow to amplify the V1-V2 hypervariable region of the 16S rRNA gene. Primers 926F and 1062R target conserved sequences flanking the V6 hypervariable region of the 16S rRNA gene (Bacchetti de Gregoris, doi: 10.1016/j.mimet.2011.06.010). Boldface indicates Illumina adapter sequences, italicized characters indicate linkers, and underlined characters indicate sequences annealing to the target gene. The sequence NNNNNNNNNNN represents the sample-specific molecular identification barcode.

Table E2. Prevalence-based contaminants

ASV[a]	Phylum[b]	Family[b]	Genus[b]	Species[b]
ASV6	Actinobacteria	Propionibacteriaceae	Cutibacterium	
ASV26	Proteobacteria	Pseudomonadaceae	Pseudomonas	
ASV156	Proteobacteria	Burkholderiaceae	Polaromonas	
ASV126	Actinobacteria	Promicromonosporace	Cellulosimicrobium	
ASV287	Actinobacteria	Nocardiaceae		
ASV321	Proteobacteria	Enterobacteriaceae		
ASV180	Actinobacteria	Propionibacteriaceae	Cutibacterium	granulosum
ASV154	Actinobacteria	Corynebacteriaceae	Lawsonella	
ASV196	Bacteroidetes	Flavobacteriaceae	Flavobacterium	
ASV326	Firmicutes	Staphylococcaceae	Staphylococcus	
ASV16	Actinobacteria	Corynebacteriaceae	Corynebacterium_1	
ASV307	Firmicutes	Streptococcaceae	Lactococcus	lactis
ASV58	Firmicutes	Staphylococcaceae	Staphylococcus	
ASV155	Proteobacteria	Burkholderiaceae	Burkholderia-Caballeronia-Paraburkholderia	
ASV661	Proteobacteria	Burkholderiaceae		

Note: [a]Numbers and corresponding [b]taxonomic assignment of ASVs identified as contaminants by the prevalence-based method implemented in decontam R package (see Supplementary Methods)

Table E3. Frequency-based contaminants

ASV[a]	Phylum[b]	Family[b]	Genus[b]	Species[b]
ASV26	Proteobacteria	Pseudomonadaceae	Pseudomonas	
ASV891	Firmicutes	Streptococcaceae	Streptococcus	
ASV2369	Firmicutes	Streptococcaceae	Streptococcus	
ASV2399	Bacteroidetes	Prevotellaceae	Prevotella 6	
ASV3041	Actinobacteria	Bifidobacteriaceae	Bifidobacterium	dentium
ASV1932	Bacteroidetes	Flavobacteriaceae	Capnocytophaga	
ASV1181	Fusobacteria	Fusobacteriaceae	Fusobacterium	
ASV292	Firmicutes	Streptococcaceae	Streptococcus	
ASV648	Firmicutes	Streptococcaceae	Streptococcus	
ASV1395	Fusobacteria	Leptotrichiaceae	Leptotrichia	
ASV900	Fusobacteria	Leptotrichiaceae	Leptotrichia	
ASV1439	Actinobacteria	Corynebacteriaceae		
ASV3055	Patescibacteria	Saccharimonadaceae		
ASV4156	Firmicutes	Streptococcaceae	Streptococcus	
ASV1585	Bacteroidetes	Flavobacteriaceae	Capnocytophaga	

Note: [a]Numbers and corresponding [b]taxonomic assignment of ASVs identified as contaminants by the frequency-based method implemented in decontam R package (see Supplementary Methods)